JOURNAL OF SPACECRAFT AND ROCKETS
Vol. 45, No. 6, November–December 2008

Summary of Hypersonic Boundary-Layer Transition Experiments on Blunt Bodies with Roughness

Steven P. Schneider*
Purdue University, West Lafayette, Indiana 47907-1282

DOI: 10.2514/1.37431

Laminar-turbulent transition on the Crew Exploration Vehicle (or Orion) is likely to be dominated by the effects of ablation and the laminar-ablated roughness, both isolated and distributed. Although no single ground experiment can simultaneously duplicate all aspects of this complex process, many experiments have been carried out using roughness applied to nonporous models without blowing. The present paper reviews these data for the effect of roughness on hypersonic blunt-body transition.

Introduction

LAMINAR-TURBULENT transition in hypersonic boundary layers is important for prediction and control of heat transfer, skin friction, and other boundary-layer properties. Vehicles that spend extended periods at hypersonic speeds may be critically affected by the uncertainties in transition prediction, depending on their Reynolds numbers. However, the mechanisms leading to transition are still poorly understood, even in low-noise environments. These mechanisms include the concave-wall Görtler instability [1], the first- and second-mode streamwise-instability waves described by Mack [2], the 3-D crossflow instability [3,4], and transient growth [5].

Nearly all hypersonic ground-test facilities suffer from high levels of noise radiated from the turbulent boundary layers on the nozzle walls. The effect of this noise on transition is often poorly understood, although it has been an issue for more than 50 years [6]. For roughness elements that are less than effective, so that transition occurs well downstream of the roughness, tunnel noise has been shown to have a substantial effect [7,8]. Quiet tunnels with laminar nozzle-wall boundary layers have been developed to provide low noise levels comparable with flight, but quiet-tunnel research has been very limited to date [9]. Recent measurements on a slender cone showed a substantial effect of tunnel noise on roughness-induced transition, even for large roughnesses that were effective under noisy flow [10].

The present review was developed for analyzing boundary-layer transition on the Orion or Crew Exploration Vehicle (CEV), a manned NASA reentry vehicle that is very similar to Apollo. The author has earlier reviewed transition on reentry capsules and planetary probes [11] (see also the other transition issues reviewed in [7,12,13]). An overall review of roughness effects on hypersonic transition was reported in [14]. The reader is encouraged to study [14] as an introduction to the present paper; the extensive introduction in that reference will not be repeated here. Earlier reviews of roughness effects on blunt bodies include those of Reda [15,16] and Batt and Legner [17]. Berry and Horvath [18] recently reviewed NASA Langley Research Center (Langley) measurements of transition induced by discrete roughness, along with recent flight data from the space shuttle. Berry and Horvath [18] described work on slender vehicles such as the X-43A, moderately blunt vehicles such as the shuttle, and blunt vehicles such as planetary probes, but only the latter are reviewed in the present paper. The present paper, revised from [19], also reviews some additional smooth-wall Apollo aeroheating data that were located after the completion of [11].

Transition on Apollo-like shapes is affected by the chemistry and mass flow of the gases blown from the ablating thermal protection system (TPS). It is also affected by the surface roughness of the laminar-ablated TPS. This is a complex problem that was comprehensively researched in the 1960s and 1970s. However, the area then fell out of favor; little has been done since the 1980s, and few of the earlier researchers are still available for comment. The author has worked almost exclusively on transition since 1985 and on high-speed transition since 1990, but even a 7500-paper library and database is far from complete; the author still has much to learn about the vast literature for high-speed transition. Since 2004, with the interest in the impending CEV, a significant proportion of the author's effort has gone toward reviewing the literature in this area, but this work is far from complete. Some experiments have looked at cold gases blown through a rough wall to simulate the flow due to ablation. Although these effects of ablation are critical and may in fact be dominant, they were reviewed separately [20]. The present review is focused on surface roughness effects.

The laminar-ablated Orion will contain two different kinds of surface roughness: 1) isolated roughness due to the compression pads, possible TPS joints, and other localized nonuniformities and 2) distributed roughness due to the laminar-ablated TPS surface. The relevant literature comes from two main sources: 1) funded research in support of Mercury, Gemini, Apollo, and the planetary probes, some of which is reviewed in [11], and 2) research funded by the U.S. Department of Defense (DOD) that investigates transition on the blunt nosetips of reentry vehicles. The problem is complex, and so most of the useful literature describes flight tests and experimental studies in ground facilities, because the computational methods available when the earlier work was done were generally primitive. These experiments are very expensive to carry out or repeat, and the budget and schedule of the Orion will only permit an effort that is much less comprehensive than the Cold War studies. Thus, the author believes it is cost-effective to review these earlier studies to identify experiments worthy of reanalysis with modern computational methods and to better plan and analyze the new experiments that should be carried out. Because a thorough reanalysis of these data is an extensive effort, this review can only serve as a beginning.

At present, the Orion is being designed using turbulent heating [18]. Isolated roughness at the service-module attachment points has been an issue, but at present these are to be designed so that they are retractable. Although transition is not currently a primary issue for the Orion design, it appears likely to arise later, as mass becomes more critical, analyses attempt to become more accurate and reliable, and more offdesign conditions are analyzed. New ground-test data for the Apollo-type geometry are being obtained as part of the Orion ground-test program (e.g., [21]); these results are not reviewed here,

Presented as Paper 0501 at the AIAA Aerospace Sciences Meeting, Reno, NV, 7–10 January 2008; received 6 March 2008; revision received 11 July 2008; accepted for publication 15 July 2008. Copyright © 2008 by Steven P. Schneider. Published by the American Institute of Aeronautics and Astronautics, Inc., with permission. Copies of this paper may be made for personal or internal use, on condition that the copier pay the $10.00 per-copy fee to the Copyright Clearance Center, Inc., 222 Rosewood Drive, Danvers, MA 01923; include the code 0022-4650/08 $10.00 in correspondence with the CCC.

*Professor, School of Aeronautics and Astronautics. Associate Fellow AIAA.

as they are well known to the community and only recently became available.

Additional Smooth-Wall Aeroheating Data for Apollo

Following the completion of [22], which became [11], additional aeroheating data were located. Because these aeroheating data had the potential to supply additional information regarding transition on Apollo, they are summarized here. However, so far, all of the data in this section appear to be laminar.

Heat-transfer measurements in the Arnold Engineering Development Center (AEDC) tunnel C with Apollo model H-1 are reported in [23]. All measurements were made on a smooth-wall model at Mach 10 and zero angle of attack. The Reynolds number based on freestream conditions and diameter Re_D ranged from $0.616–1.480 \times 10^6$. Although Re_D is not necessarily the best parameter to describe the flow, it can be obtained readily without sophisticated computations, and so it is often the only Reynolds number available. There was apparently a problem with nonuniformity of the tunnel centerline flow, as determined by comparisons with Lees's [40] laminar theory. However, it appears that the data are all laminar.

Apollo aeroheating measurements were also obtained in a shock tunnel at NASA Ames Research Center (Ames) at high enthalpy [24]. The Mach number was 10 and the angles of attack ranged from 0 to 44 deg. However, the Reynolds number was only $60,000/\text{ft}$ in the freestream, with models that were 2.5 in. in diameter, and the data are apparently all laminar. Afterbody separation began near a 23 deg angle of attack (AOA), and the flow over most of the windward surface was attached at a 33 deg AOA.

Miller and Lawing [25] measured heat transfer to Apollo in the Langley hot-shot tunnel at Mach 20 in nitrogen. However, $Re_D \simeq 1 \times 10^5$, and the flow was apparently again all laminar. The flow is again attached along the windward meridian at 33 deg AOA. At zero AOA, it separates on the afterbody at an arc length to a model radius ratio of about 1.4.

Lee and Sundell [26] measured heat transfer to Apollo in an arc jet at Mach 13.8. The afterbody flow was separated at zero AOA and attached on the windward side at 33 deg AOA. The flow was apparently all laminar, probably because $Re_D \simeq 800$. The data are plotted against measurements from several other high-enthalpy facilities and all appear to provide laminar flow.

Lee and Sundell [27] later measured afterbody heat transfer to Apollo in an arc jet at Mach 5.8 to 8.3. The model was 0.0065 scale and had a Teflon nosecap to study ablation effects. The flow was almost certainly laminar, because $Re_D \simeq 200–22,000$. Afterbody heat transfer decreased by a factor of 2 with ablation.

Kemp [28] measured afterbody pressures on Apollo in the helium tunnels at Ames at Mach 10 to 21 and in air at Mach 14. In helium, $Re_D \simeq 0.036–1.15 \times 10^6$, and in air, $Re_D \simeq 11,800$. Free-flying telemetered measurements were made to avoid sting-support interference. Although transition is not discussed, it appears that the data are all laminar.

Akin [29] measured heat transfer to Apollo in a combustion-driven shock tunnel using both air and carbon dioxide. The Reynolds numbers are not given, but the stagnation pressure was 285 atm and the freestream velocity was 12 kft/s in CO_2 and 13 kft/s in air. There is no evidence of transition in the heat-transfer distributions on the blunt face, despite the substantial stagnation pressures. It would be interesting to see some further analysis to understand why transition apparently did not occur.

Gorowitz [30] measured heat transfer to a 0.01875-scale Apollo model in the 12-in. shock tunnel at North American Aviation at Mach numbers 15.5, 16.8, and 18.3. The AOA ranged from zero to 40 deg. The geometry was from a preproposal stage and did not duplicate the final geometry. The full-scale diameter was 160.0 in., with a 192.0 in. blunt-face radius, a 35 deg afterbody half-angle, and an 8.0 in. toroidal radius at the junction between the blunt face and afterbody. Pressure and heat-transfer data were tabulated at unit Reynolds numbers of $1.64–2.67 \times 10^5/\text{ft}$, depending on Mach number. Ten thin-film gauges were used on the model. Because the model diameter was 3.0 in., $Re_D = 0.41–0.67 \times 10^5$, and the data are probably all laminar. Comparison data were also obtained on a 1.75-in.-diam sphere.

Additional Ballistic-Range Data for Apollo

Following the completion of [22], additional ballistic-range data were located. Because these data had the potential to supply additional information regarding transition on Apollo, they are summarized here. However, so far, all of the data appear to be laminar.

DeRose [31] measured lift, drag, and trim on Apollo capsules in the Ames ballistic range at high Mach numbers, including the use of the counterflow shock tunnel. The report contains three shadowgraph images at $Re_D = 52,500–214,000$. DeRose made shots to $Re_D = 3.06 \times 10^5$ at Mach 11.2 (run 1512). If these shadowgraphs can be retrieved with good quality, they might shed light on transition on the afterbody and in the wake. Unfortunately, no NASA Ames photo numbers are given, and so there is no known archive for such photos.

Sammonds [32] measured forces and moments on Apollo capsules and slightly modified shapes in the ballistic range at Ames at Mach numbers from 5 to 35. The counterflow shock tunnel was also used, yielding $Re_D \simeq 40,000–350,000$. No effect of Reynolds number was observed in the force and moment data, suggesting that they were all laminar. Thirteen shadowgraphs are included and these are said to show transition moving forward in the wake as the Reynolds number increases. However, the electronic images from the NASA Science and Technical Information (STI) center are not good enough to see clearly. The original images might be helpful for understanding wake transition. However, the photos do not include any archival image numbers, which suggests that the originals are probably lost. The density is low due to the high Mach number, the small models were only 1 cm in diameter, and so the resolution of the shadowgraphs will be much less than in some of the supersonic-range images.

Lawrence and Norman [33] measured forces and moments on Apollo capsules in range G at the AEDC. The Mach numbers were 6 and 8.5, and $Re_D = 50,000–240,000$. The focus of the tests was on resolving anomalies in low-Reynolds-number aerodynamics between the AS-202 flight and previous ground tests. The data are probably all laminar, and there is no discussion of transition. Shadowgraphs were obtained but none were shown. It is not clear if any were archived.

Isolated Roughness Effects on Apollo Transition

There are very few studies of the effect of isolated roughness on transition on hypersonic or supersonic blunt bodies. Public-release flight data for transition on blunt bodies are reviewed in [12]. Blunt bodies are difficult to study in ground experiments, because blunt models must be relatively small if their strong bow shocks are not to unstart the wind tunnel. Few facilities can achieve sufficiently high Reynolds numbers to study transition on blunt bodies, and these tend to be expensive. Most of the DOD interest has been in uniformly ablating nosetips. Most studies of the effect of isolated roughness have been carried out for two purposes: 1) determining the local heating around isolated roughnesses or 2) using rows of isolated roughnesses for tripping purposes. Thus, any transition data were usually obtained as a byproduct.

Effect of Protuberances on Apollo Heating

Bertin [34] summarized the wind-tunnel data for protuberance and cavity effects on Apollo heating, as is also discussed in [11]. The smooth-wall data are also reviewed. However, there is no explicit discussion of transition. With the computational methods available in 1966, it would have been nearly impossible for Bertin [34] to distinguish interference heating and vortical-wake heating from heating induced by transition in the wake of the protuberances and cavities.

Bertin [34] collected previously reported data from the Ames and Langley tunnels. He also reports new data from tunnel C at AEDC and from the 21-in. hypersonic tunnel at the NASA Jet Propulsion Laboratory (JPL). Bertin reported the use of a 0.045-scale Apollo model in tunnel C for smooth-wall heat transfer and a 0.090-scale model for heat transfer near cavities and protuberances. The 0.045-scale data are reported in detail in [35] and appendices. The 0.090-scale data appear to be the same as those reported in 1069-page detail in [36]. The pretest report contains additional information on the tunnel C experiment [37]. An 0.02-scale model was tested at JPL; the basic data are reported in [38,39].

Figure 1 sketches the protuberances and cavities in the Apollo command module. Bertin [34] stated that the full-scale shear pads are 6.5 in. in diameter and protrude 0.55 in. above the surface. The full-scale scimitar antenna is 2.1 in. wide and extends a maximum of 8.1 in. above the surface. The full-scale umbilical fairing protrudes 3.1 in. above the surface. The windward tower well is a cavity 14.8 in. long by 5.5 in. wide with a maximum depth of 4.6 in.

According to [36], the full set of blunt-face protuberances is larger than those shown in Bertin's [34] approximation. Figure 2 shows 3 compression pads, 3 shear pads, plus an oxidizer dump, whereas Fig. 1 shows only the 3 shear pads. Recall that the tunnel C model was 9% scale. Some of the tunnel C models shown in [36] also show blunt-face ramps leading to the umbilical fairing. The tunnel C models were 0.02-in.-thick 310 stainless with 294 thermocouples welded on the inside. Note that the 9.0% model was 6.930 in. in radius (Fig. 2). Per the imperfectly reproduced foldout drawing at the end of [37], the compression pads were centered 5.332 in. from the model center, with a diameter of 0.54 in. Two of the compression pads had a thickness of 0.045 in. and one was 0.099 in. The oxidizer dump was 0.445 in. in diameter, 0.009 in. thick, and located at a radius of 6.164 in. The shear pads are located at the same radial location as the compression pads; although some detail is shown on the foldout drawing, it is difficult to read. However, the shear pads include some kind of 3-D protrusion at a radius of 5.675 in. that protrudes 0.150 in. at a 37.85 deg angle. Thus, there seem to be some unexplained contradictions between Bertin's [34] summary and some of the details in the source reports. Emerson [36] plotted and tabulated over 1000 pages of heat-transfer data from several different configurations.

Bertin [34] noted that the laminar heating on the smooth configuration was essentially independent of flow conditions and test facility. Bertin compared the pressure measurements to Newtonian values, which was all he had available. The smooth-wall heating measurements were compared with Lees's [40] well-known laminar theory. The tunnel C measurements were carried out at $Re_D = 0.2–1.2 \times 10^6$, and the JPL measurements were carried out at $Re_D = 0.17–0.62 \times 10^6$; both of these values are fairly low. Emerson [36] gave the tunnel C freestream Reynolds number range as 0.33 to 2.0 million per foot, with a 13.86-in.-diam model. Bertin [34] plotted heating rates normalized by the value at the stagnation point at zero angle of attack. The smooth-wall data appear to be laminar, because they agree fairly well with Lees's [40] laminar theory.

Bertin [34] presented the heating data as a ratio to the value measured on a smooth model at the same location, calling these *interference heating factors*. Interference factors in the wake of shear pad 1 ranged from a typical 1.5 to as high as 2.7, possibly due to transition or possibly to vorticity in the wake. Because this pad was in a subsonic region, there was no shock/boundary-layer interaction, and the heat transfer was unaffected upstream of the pad.

Upstream of the shear pads in the supersonic region, interference heating factors were as large as 8, probably due to shock/boundary-layer interactions. The effect of Reynolds number on the interference factors depended on the location studied, and so Reynolds number effects cannot be easily used to infer transition. However, in the wake of shear pad 1, the interference factors consistently rose with Reynolds number. A detailed reanalysis would be necessary to establish a clear physical cause for this effect.

Bertin [34] stated that the height of shear pad 3 is about twice the momentum thickness in the incoming boundary layer ([34], page 13). Thus, these protuberances are nontrivial.

Effects of Apollo Surface Cavities and Protuberances on Heating

Jones and Hunt [41] measured heat transfer to the Apollo command module in the Mach-8 tunnel at Langley using phase-change paint. Heating increases were measured near the shear pads, umbilical fairing, reaction control jets, and antenna for $Re_D = 0.13–1.5 \times 10^6$. The models were 4.00 in. in diameter, the shear pads were 0.016 in. high, and the adjacent tension ties were 0.040 in. high. The heating increases were analyzed in terms of interference factors, as in [34]. If transition occurred in the wake of the roughness elements, there was no way for Jones and Hunt [41] to distinguish it from vortex-induced heating, and there was no discussion of transition.

Hunt and Jones [42] reported more measurements of a similar type, 3 years later. It is again difficult to see if any of the roughnesses

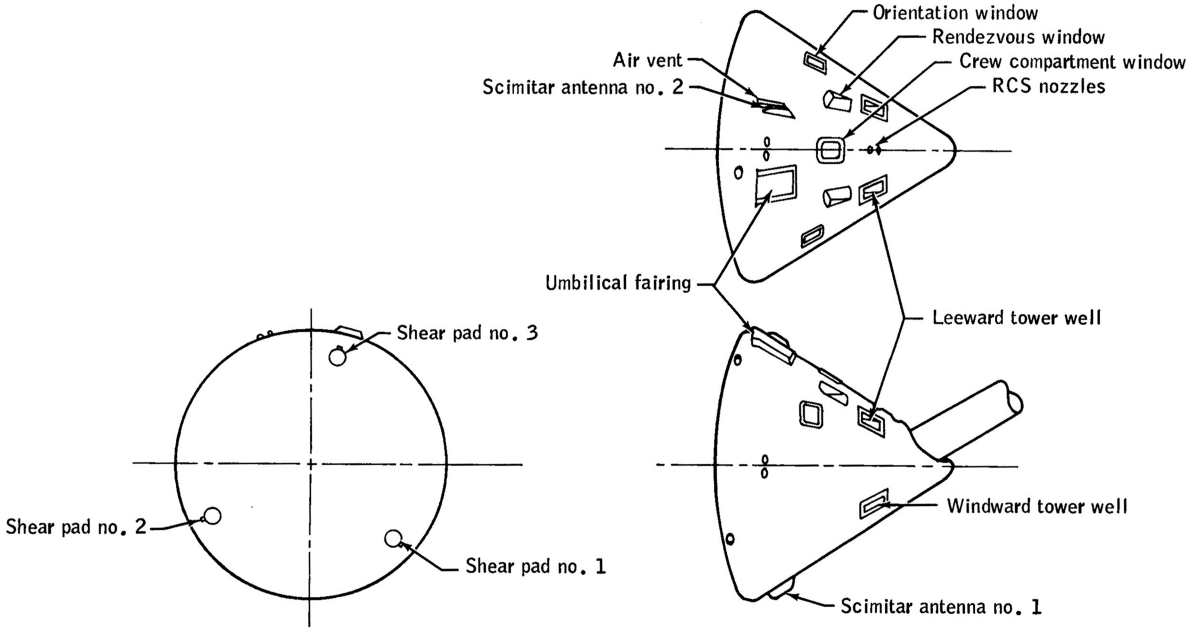

Fig. 1 Sketch of the Apollo command module illustrating the cavities and protuberances (from [34], Fig. 2) (RCS denotes reaction control systems).

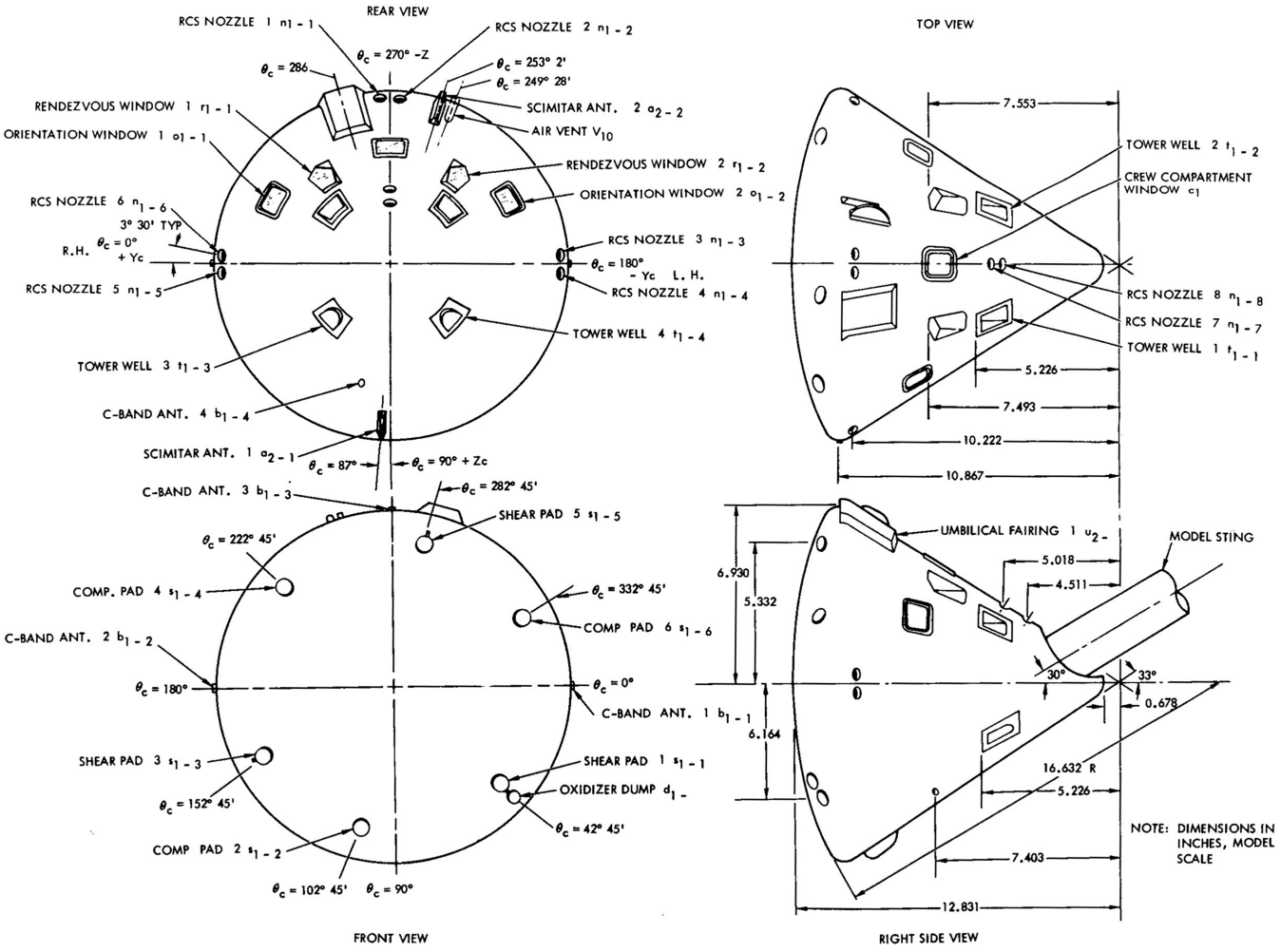

Fig. 2 Sketch of the H-11 heat transfer model of the Apollo airframe 011 command module illustrating the cavities and protuberances (from [36], Fig. 1).

induced transition, for similar reasons. Figure 26 in [42] appears to show transition on the afterbody as the Reynolds number is increased, but the authors do not believe it is due to transition because the rise begins at the same location, independent of Reynolds number.

Jones and Hunt [43] also summarized these measurements. However, this document does not appear to contain any additional information that is useful for the present purpose.

Catalog of Apollo Tripping Experiments

Apollo models used to obtain data with isolated tripping roughnesses were summarized in [44]. The entire Apollo wind-tunnel program was summarized in [45,46]. Fifteen trip configurations were designed and tested; configurations 7 to 10 and 13 to 15 involve trips on the blunt spherical face, and the rest involve trips on the conical afterbody for launch studies. Configuration 7 is shown in Fig. 3. It appears that the stagnation point on the blunt face at the nominal angle of attack of about 33 deg is expected near the upper center of the face, and so the tripping spheres are located in a semicircular arc downstream of this stagnation point. Configuration 7 was tested in AEDC tunnel B using model H-2, as documented in the North American Aviation's Space and Information Division (SID) report SID 62-993. Biss and Emerson [35] documented 7 runs with trip 7 at unit Reynolds numbers of 0.0833×10^6/in. and 0.30×10^6/in. and at angles of attack of 28 to 40 deg.

Configuration 8 was similar except that the sphere diameter was increased from 0.694 to 1.042 in. in diameter (full scale) and the arc of trips was located farther from the stagnation point. It was also tested on model H-2 in tunnel B in 11 runs at zero AOA and unit Reynolds numbers varying from 0.0364×10^6/in. to 0.295×10^6/in. [35].

Configuration 9 was similar to configuration 7 except for the radii of the arc of trips. It was tested twice on model H-2 in tunnel C, as apparently reported in SID 62-993, SID 62-1214, and SID 63-688. Biss and Emerson [35] report 8 runs at AOA ranging from 28 to 40 deg and unit Reynolds numbers of 0.0833×10^6/in. and 0.200×10^6/in.

According to [35], "Flow transition over the entry face of the command module was achieved, and its effect on the heat transfer distribution was shown. Flow transition on the afterbody of the command module was not attained." These data are to be discussed further subsequently, although reanalysis will be required.

Configuration 10 changed to the use of grit trips, as shown in Fig. 4. Configuration 10 was tested in the JPL hypersonic tunnel on model H-1 during test JPL 21-102, as apparently reported in SID 62-354 and SID 62-628. See the subsequent discussion of [38,39] (SID 62-628); the critical data from this test appear to lie in pages that are missing from the end of volume 2 of this report, and the search for pages A-1221 to A-1419 continues. SID 62-354 remains to be located.

Configuration 13 also uses a band of grit on the blunt face and was tested in the Langley Unitary Plan Wind Tunnel on model H-2, as reported in SID 62-1011 and SID 63-683. The reference to SID 63-683 in [46] is a typo, as this report number does not contain Apollo heating data.[†] Experiments with configuration 13 are apparently not reported in the open literature.

[†]Private communication with Garland Gouger, NASA Langley Research Center library, 21 August 2006.

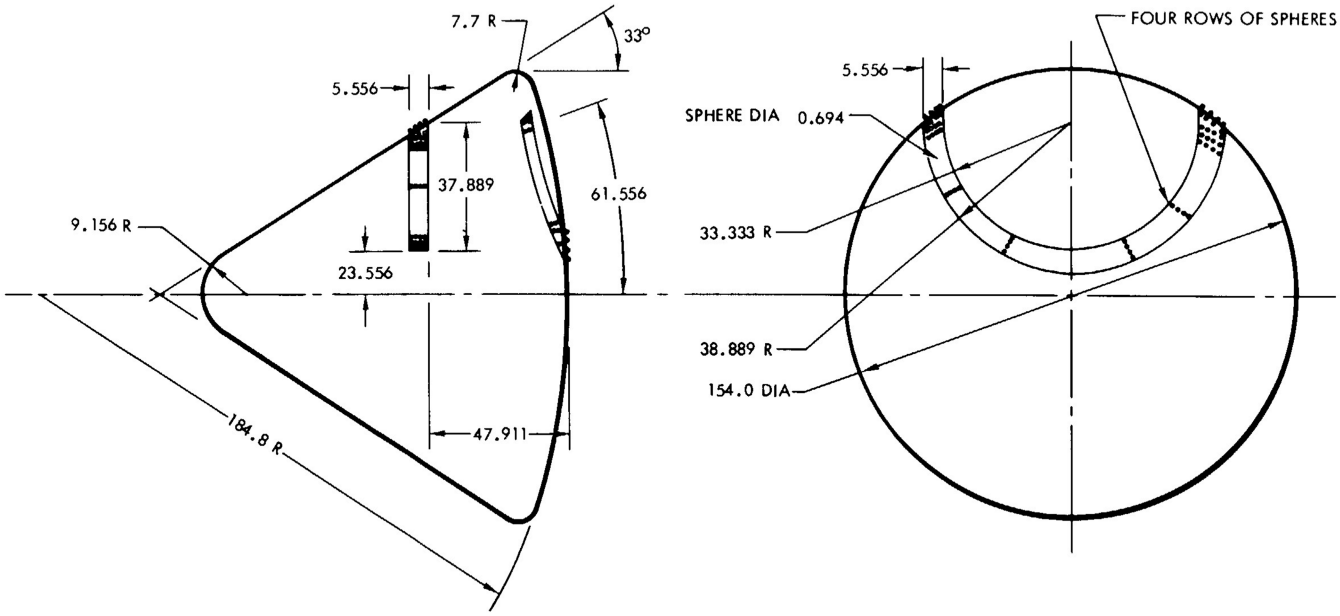

Fig. 3 Sketch of the Apollo command module illustrating boundary-layer tripper no. 7; full-scale dimensions are in inches (from [44], page 22-9).

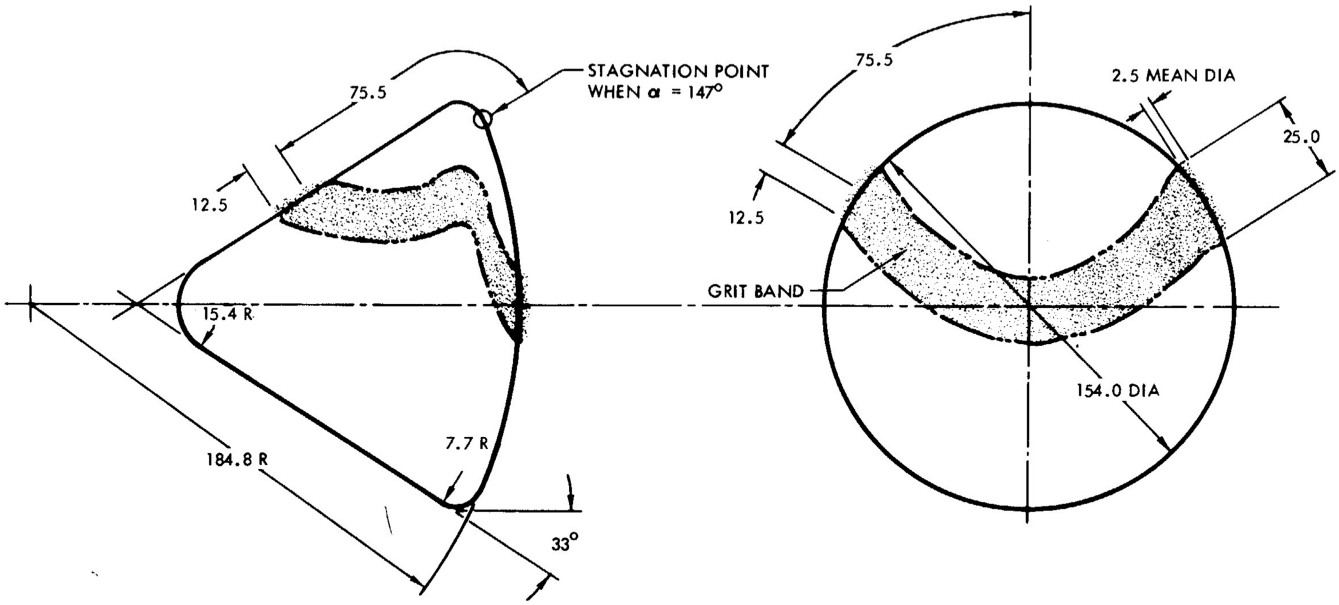

Fig. 4 Sketch of the Apollo command module illustrating boundary-layer tripper no. 10; full-scale dimensions are in inches (from [44], page 22-12).

Configuration 14 was tested on model H-2 in tunnel C, as apparently reported in SID 62-1214 and SID 63-688. It uses four rows of staggered spheres in a similar arc band. There is a second band on the afterbody. Measurements on this configuration are not reported in the open literature either.

Configuration 15 was tested on model H-2 in tunnel C, as reported in SID 63-1135 [47]. It uses spherical balls distributed uniformly over the blunt face, except near the centerline. Trip configurations 15 and another numbered 16 were tested in AEDC tunnel C, as reported in [47]. Trip configuration 15 was tested at freestream Reynolds numbers ranging from 0.083–0.166 $\times 10^6$/in. and angles of attack ranging from 40 to 20 deg. The run summary shown in Table 5 of [47] does not show any runs with configuration 16, nor are any further details reported for this configuration. Figures 6 and 7 in [47] include photographs of the trips, but the electronic images provided by NASA STI are unreadable. Reference [48] contains plotted data for the tripped conditions on pages A-776–A-925. This large volume of plotted data would have to be reanalyzed to determine if transition was successfully tripped, under what conditions, and where. Reference [49] contains tabulated data for these conditions on pages B-690–B-789. The tabulated data are legible and could be typed into files or possibly machine scanned.

Some of these studies contain data that show the conditions under which these trips were effective in causing transition on the blunt face. These cases provide data for the effect of controlled roughness on transition under wind-tunnel conditions. A reanalysis of these data appears warranted, but computations of the mean flow for a capsule at angle of attack are still not trivial.

Effect of Rows of Sphere Trips on Apollo

As cataloged previously, Biss and Emerson [35] measured tripped transition on the blunt face of Apollo in tunnels B and C at AEDC. The 0.045-scale models were instrumented with 98 thermocouples

on the back of the 0.040-thickness stainless-steel skin. The plots are found on pages A-182–A-195 for the tunnel B data and pages A-636–A-651 for the tunnel C data ([35], page 10). Biss and Emerson [35] stated that "It appears from the curves that boundary-layer transition was achieved downstream of the trips on the entry face but not from the trips on the afterbody. The runs made at higher Re/in. in both tunnels showed a more pronounced variation. . ." in heating. Per the run summary, the plotted tunnel B data were all obtained with trip configuration 7, although both configurations 7 and 8 were used as part of AEDC configuration 31. The trip 8 data were obtained with the model offcenterline. The plotted tunnel C data were all obtained with trip configuration 9, which is again labeled AEDC configuration 31.

The tunnel C data with AEDC configuration 31, trip 9, for groups 33 to 40 are plotted on pages A-636–A-651 of [50]. There were 4 runs at a unit Reynolds number of 0.0816×10^6/in. and four at 0.1999×10^6/in. The angle of attack ranged from 48 to 28 deg. The data would have to be reanalyzed to see what can be learned from them and compared with the smooth-wall data. However, all of the data appear to show tripping, and so the onset of a tripping effect is not obviously present. The tunnel C data for trip configuration 9 are tabulated on pages B965–B1003 of [51], groups 33 to 40. The unit Reynolds number is $0.0816–0.199 \times 10^6$/in. for AOA ranging from 28 to 48 deg, and so these tabulated data appear to be the same data plotted in [50].

The tunnel B data with trip configuration 7 in groups 79–82 are plotted on pages A-182–A-195 of [52] and tabulated on pages B394–B413 of [53]. The data were plotted for unit Reynolds numbers of 0.0808×10^6/in. and 0.2962×10^6/in. for AOA ranging from 28 to 40 deg Most of the tabulated data appear legible. Comparing the plots for the high and low Reynolds numbers for the 33 deg AOA case, pages A-187 and A-193 of [52], some azimuthal rays appear to show the onset of transition with the increase in Reynolds number. For example, the 0–180 deg line appears to show transition at $s/R \simeq -0.6$. However, the high heating that seems to be due to transition shows up only on one thermocouple along this ray, which might therefore be some sort of instrumentation error. The data need to be replotted and reanalyzed to determine if and where transition occurs. The level of definition supplied in the report is not sufficient to make this a simple process.

The tunnel B data with trip configuration 7 for groups 83 to 85 are tabulated on pages B416–B430 of [54]. The freestream unit Reynolds numbers are all 0.2962×10^6/in. and the AOA ranges from 28 to 40 deg. It appears that these tabulated data supplement and do not duplicate the plotted data, which will have to be digitized. The tunnel B data with trip configuration 8 for groups 133 to 143 is tabulated on pages B669–B723 of [54]. The freestream unit Reynolds number ranges from $0.0364–0.294 \times 10^6$/in. in five steps, which may allow determining the Reynolds number variation. The angle of attack is zero for the data with trip 8. These data would have to be analyzed with care to determine the thermocouples behind the arc of trips.

Distributed Roughness Effects on Apollo Transition

Effect of Grit Tripping Strip on Apollo

Fromm [38,39] described tests of a 2.0% scale model of the smooth Apollo command module in the hypersonic wind tunnel at JPL. The full-scale dimensions were a 154 in. diameter, 184.8 in. radius of the spherical end, 7.7 in. corner radius, 33.0 deg afterbody half-angle, and 15.4 in. afterbody vertex radius. A thin-skin model was used, with thermocouples welded on the inside. The model included five rows of thermocouples and a total of 44. The model diameter was 3.08 in. and was tested at Mach numbers ranging from 6.0 to 9.0 and $Re_D = 0.06–0.8 \times 10^6$. The grit height was 0.05 in., distributed over a band 0.5 in. wide, with the center of the band at 1.51 in. from the stagnation point ([38], page 8). Unfortunately, it appears that the model with the grit was only tested at Mach 6, a 33 deg angle of attack, and Re_D of 0.616×10^6 and 0.800×10^6. A shadowgraph was reported to show the effect of the transition grit, but the image is unreadable in the electronic copy from NASA STI.

The data from the brief tripping study were obtained in runs 88 and 89. The run conditions are described in volume 1, but the actual heat-transfer data are not there, nor in volume 2, which ends at page A-1220, and the table of contents lists A-1419 as the last page. The search for pages A-1221–A-1419 continues. Unfortunately, neither JPL nor NASA STI nor the NASA Langley library seem to have copies, and so these data may be lost.

Previous Reviews of Transition on Blunt Models

Transition on blunt nosetips was a major DOD concern through the 1970s. Well-known reviews of this case were developed by Batt and Legner [17] and Reda [15]. The Passive Nosetip Technology (PANT) program was undertaken to understand the related issues; although many of these reports are still for limited distribution, some are for public release [55–57]. The roughness generated by laminar ablation is generally not much larger than the boundary-layer thickness; much larger roughness can also be generated by ablation, apparently only after the boundary layer has become turbulent [58].

Excellent photographs of the laminar-ablated surface roughness of 24 typical nosetip materials were reported by Eitman and DeMichaels [59]. Examples of these images are shown in Figs. 5–7. These images are for a sample nosetip made of fine-weave pierced fabric (FWPF) with a 1.00-in.-diam nose, ablated in the 50 MW arc jet that once operated at the U.S. Air Force Flight Dynamics Laboratory at 76 atm in the ramp mode, with peaked enthalpy. Laminar ablation flattens out the nosetip geometry, as shown in Fig. 5. Many studies were carried out to determine the effect of transition on ablation-induced changes in the nosetip geometry, but it

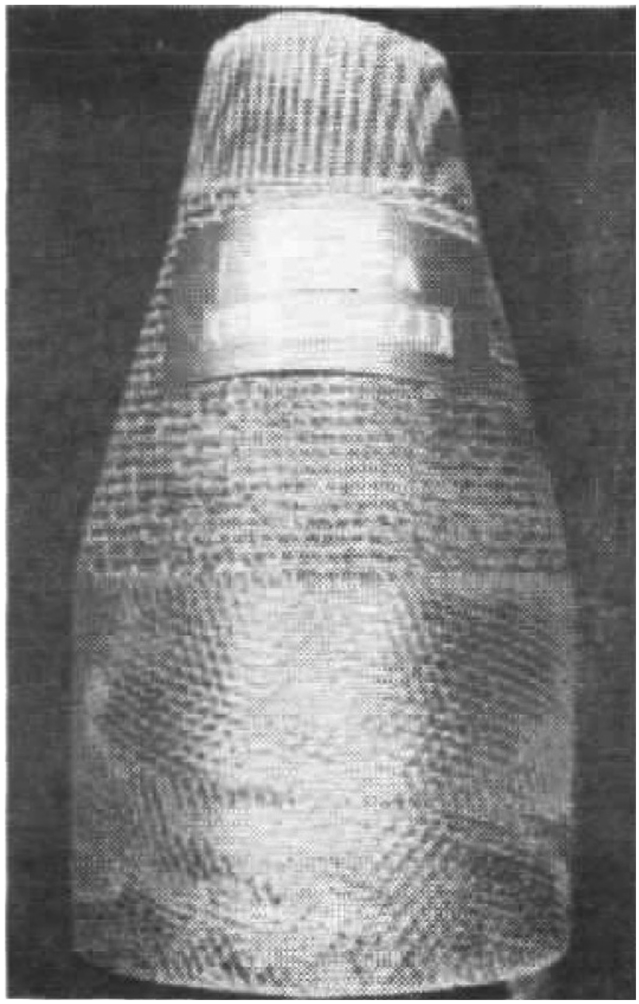

Fig. 5 Side view of the laminar-ablated FWPF nosetip (from [59], Fig. 77).

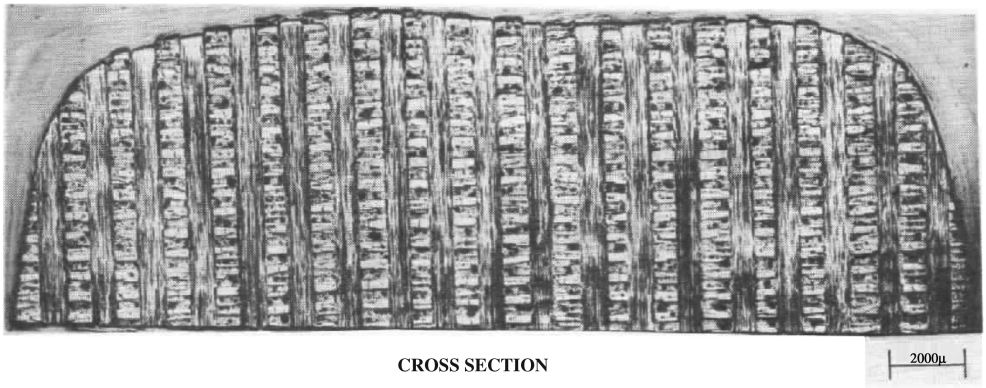

Fig. 6 Cross section of the laminar-ablated FWPF nosetip (from [59], Fig. 77).

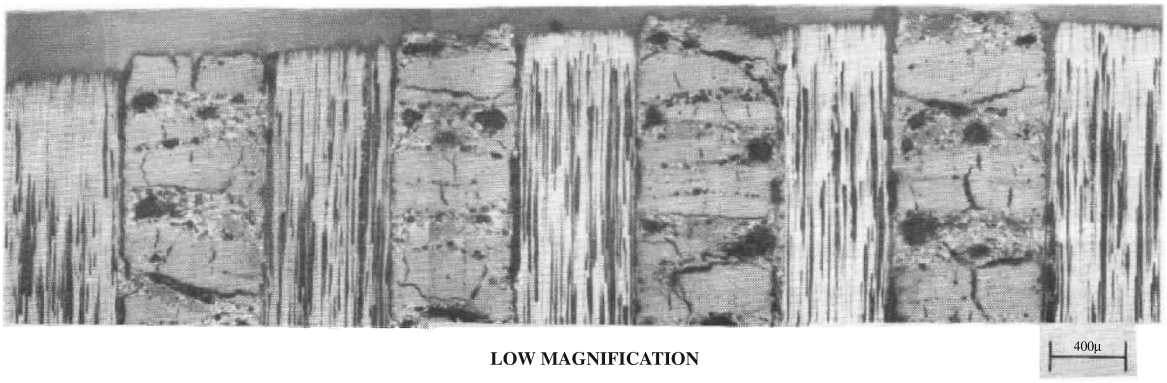

Fig. 7 Low-magnification image of the laminar-ablated FWPF nosetip (from [59], Fig. 77).

seems generally accepted that fully laminar nosetip ablation at a zero angle of attack just serves to flatten out the nosetip shape.

The model is then sectioned, vacuum-mounted in thermosetting plastic, and polished. Figure 6 shows a cross section. The vertical Z yarns of the woven carbon–carbon can be clearly seen; these ablate at a faster rate than the matrix and transverse yarns, causing a characteristic pattern in the surface roughness. The scale of the image is shown in the lower right of Figs. 6 and 7; the vertical Z yarns are roughly 1.3 mm apart.

Under low magnification in Fig. 7, the surface roughness can be seen more clearly. Microroughness measurements were made on the Z yarns (mean of 0.98 mil), the transverse yarns (0.18 mil), and the matrix pockets (0.42 mil). The peak microroughness height for this material was of the order of 1.5 mil ([59], Fig. 35). The median macroroughness height was 3.0 mil ([59], Table 6); this value considers the regular pattern of peaks and valleys corresponding to differential ablation between the yarns and the matrix. The peak macroroughness height was of the order of 6–8 mil ([59], Fig. 56). Eitman and DeMichaels [59] also measured the porosity and other properties of these composites; as is evident from their discussion, it is not certain which characteristics of the roughness have the largest effect on nosetip transition in flight. The largest roughness in a surface usually causes the earliest transition downstream, but an average roughness is usually used to characterize the roughness of nosetip materials.

The blunt-body paradox refers to the paradoxical early onset of transition on nominally smooth blunt bodies, for which the favorable nose-region pressure gradient and low wall temperatures were expected to produce laminar flow. It appears that Morkovin [60,61] coined the term. Stetson [62] provided the most recent review of this topic (see the discussion of the related public-release flight data in [12]). The Mark-2 [63] and X-17 [64,65] data sets are the most well known. Most of the flight data for these vehicles are still classified or limited.

Wisniewski [66] reviewed highly cooled blunt bodies in 1960. He correlated transition using a Reynolds number based on displacement thickness and the ratio of wall to total enthalpy. Although he notes that ". . .cooling may cause the boundary layer to go from laminar to turbulent flow," he does not evaluate roughness effects, which the present author believes is the most likely mechanism for this effect. Nevertheless, his discussion and list of references are useful.

Potter and Whitfield [67] wrote a brief discussion of the effects of cooling and roughness in 1961. They showed that surface roughness in previous experiments could explain the reversal of the movement of transition with wall temperature, if a (proposed) different correlation is used. This shows the importance of treating a wide variety of data with a systematic comparison of correlations, which, of course, takes a substantial effort. Unfortunately, substantial efforts of this type have been all too rare, perhaps because they fall into a gap between basic research and vehicle development.

Abbett et al. [56] reviewed the literature for the PANT program in 1975. Smooth-wall blunt-body transition was of particular interest, and the flight data from the Mark 2, X-17, and NACA programs were discussed. The PANT correlation was generalized for blowing due to ablation [55].

Finson et al. [68,69] wrote another review in 1976–78. Finson et al. believed that Re_k correlated the data better than k/θ and preferred to include a curvature term. Here, Re_k is a Reynolds number based on the roughness height k and conditions in the undisturbed boundary layer at the roughness height, and θ is momentum thickness. Finson et al. provide a good summary of the limitations of the available data and the difficulties in using any of the correlations.

Ground-Test Experiments for Transition on Other Blunt Models

Although ground-test data for supersonic and hypersonic transition on very blunt models is relatively scarce, considerable

data do exist. The following summarizes the public-release literature in this area, in chronological order.

Cones and Hemispheres at Mach 4 and 8 in the Ballistic Range

Seiff et al. [70] measured transition on blunt cones, hemispheres, and spheres in the Ames ballistic range at Mach 4 and Mach 8. The Mach-4 experiments should have low noise, but the Mach-8 experiments used a counterflow wind tunnel and therefore suffered from visible levels of noise in the shadowgraphs. The basic model was a 60 deg included-angle blunt cone, with a base radius of 0.863 in. and a nose radius of one-third of the base radius. Measurements were also made on a 60 deg included-angle sharp cone, a hemisphere with a 0.863 in. base radius, and a $\frac{3}{8}$-in.-diam sphere. Three levels of surface finish were used and characterized with interferograms. Transition was inferred from spark shadowgraphs.

For the blunt cones with the least polish at Mach 8.3 and $Re_D = 4.8 \times 10^6$, transition was often asymmetric, with the turbulent side remaining the same regardless of whether it was windward or leeward. This was taken as being due to the variability in surface roughness. The highest polish did not increase the amount of laminar flow, perhaps because it was still too rough.

The sharp cones were laminar to an arc-length Reynolds number of 6.7×10^6 at Mach 8.3, with a similar finish. Seiff et al. [70] concluded that bluntness increased the sensitivity of transition to surface roughness; this conclusion is generally consistent with later observations by Stetson [72], although the scaling and mechanism remain to be understood ([13], Sec. 4.4.1). The hemispheres with the coarsest finish appeared to become turbulent at Mach 8 at an arc-length Reynolds number of 20,000. At the low-noise Mach-4 condition, transition began at an arc-length Reynolds number of less than 800,000. Because the hemisphere shadowgraphs were difficult to interpret, the results are uncertain.

Seiff et al. [70] analyzed the roughness height at the stagnation point and determined it to be roughly 1% of the boundary-layer thickness, which was thought to be sufficient to have a substantial effect on transition. It would be very good if the original shadowgraphs could be recovered for reanalysis. However, it appears that nearly all of the shadowgraphs from the Ames range have been lost, except for those that are numbered in the reports and were therefore saved in the Ames photo archive (see the discussion in [11]).

These results are worthy of further analysis, although many of the details have been lost. Further ballistic-range experiments of this type should be considered, because they can have the advantage of being free of tunnel-wall radiated noise, when the counterflow is absent.

Two-Inch Hemispheres at Mach 5

Cooper and Mayo [71] measured transition on 2-in. hemispheres in a Mach-5 open-jet wind tunnel at Langley for unit Reynolds numbers as high as 77.4×10^6/ft. The hemispheres were polished to 10–20 μin., but the polish degraded under the pitting action of impinging particulate. This problem is common, as discussed in [72], although often it goes unrecognized or unmentioned. Although the pits were polished between runs, the original surface finish could not be maintained. However, data were carefully taken almost immediately after the model was first introduced into the flow. The thin-skin models were instrumented with 6–8 backside thermocouples. The original smooth models were laminar to $Re_D = 12.1$–12.9×10^6 or freestream unit Reynolds numbers of 72.6–77.4×10^6/ft. After the test the model contained pits about 0.002 to 0.003 in. in diameter. When these pitted models were tested without repolishing, transition occurred at $s/R = 0.35$, where s is the arc length from the stagnation point and R is the radius of the sphere. The ratio of wall temperature to stagnation temperature was typically 0.53 to 0.66.

This test shows that very high transition Reynolds numbers can be obtained on blunt models if the surfaces are highly polished. It also shows the sensitivity to small roughness. Both of these remarks are in general agreement with flight data [12], despite the difference in freestream noise levels. Unfortunately, the pitted roughness properties were not measured, and so the test does not provide any data relating roughness height to transition location.

Nineteen-Inch Hemispheres at Mach 2.48 to 3.55

Bandettini and Isler [73] measured transition on 19.02-in.-diam hemispheres in the 8 by 7 ft Unitary Plan Supersonic Tunnel at Ames. The initial surface roughnesses were 50, 580, and 2760 μin., and unit Reynolds numbers ranged from 0.96–4.78×10^6/ft. Tunnel freestream particulate caused pits on the 50 μin. hemisphere, ranging in depth from 1500 to 2500 μin. Transition was determined from shadowgraphs or thin-skin thermocouples. Most of the data were obtained at Mach 3.07. Before the appearance of these pits, the smooth hemisphere was laminar to 90 deg from the stagnation point (the last station) to $Re_D = 7.57 \times 10^6$ and $Re_\theta = 660$. At these high Reynolds numbers, the pitted smooth model or the rougher models showed transition at about 50 deg from the stagnation point. A page of tabulated data is presented to show the location of transition for the various rough models at various unit Reynolds numbers, and a good description is given for the model roughness and how it was characterized. The data appear worthy of reanalysis with modern approaches.

Two-Inch Cold Hemispheres at Mach 5

Cooper et al. [74] later measured transition on 2-in. cooled hemispheres at Mach 5 and a freestream Reynolds number of 73.2×10^6/ft. The stagnation temperature was about 400°F, and the initial ratio of wall temperature to freestream stagnation temperature varied from 0.16 to 0.65. Thin-skin models with backface thermocouples were used to infer transition. The initial wall temperature was either 100°F (room temperature) or −320°F (liquid nitrogen). The model roughness was 2–3 μin. rms with isolated scratches and pits with depths of about 10–20 μin.

The test with the hot wall was in essential agreement with the earlier measurements [71]. Transition on the hot model "...resulted from surface roughness caused by the impact on the model surface of small particles in the airstream." Pits of 0.005 in. in diameter were commonly observed under a 40-power microscope. The rim of the pits was probably surrounded by a raised edge, and raised edge heights of 1/10 of the diameter were suggested as a reasonable possibility. "During two of the four cold tests, the boundary-layer flow changed from turbulent to laminar over large regions of the hemisphere as the model heated." Cooper and Mayo [71] did not believe this was a roughness-related effect, based on simple Re_k estimates, but the present author [13] believes this data could be analyzed as a roughness-induced effect, similar to the one observed by Stetson [72]. As the model heats up, the boundary layer thickens, and the relative height of the roughness decreases. Further analysis appears warranted.

Sphere Ellipsoids at Mach 3

Deveikis and Walker [75] measured transition on roughened sphere ellipsoids at Mach 3 in the Langley 9 by 6 ft thermal structures tunnel at $Re_D = 2.76 \times 10^6$ and $Re_D = 4.25 \times 10^6$. The radomelike models had a nose radius of 2.25 in. and were tested with surface roughnesses of 5, 100, and 200 μin.. The thin-skin models were instrumented with backface thermocouples, which were used to infer transition location.

Transition onset locations varied from $s/D = 0.1$–0.5, where s is the arc length from the stagnation point and D is the model diameter. The surface finish on the 5 μin. model degraded by only 20 μin. after the test, because efforts had been taken to reduce airstream contamination. With the 5 and 100 μin. models, data was only obtained at the higher Reynolds number, due to instrumentation breakdowns. Transition was promoted by surface roughness and boundary-layer cooling. Transition on the rough models was delayed when they were heated. These measurements should be

recomputed with modern methods to compare them with various correlations.

Blunt Noses at Mach 2.2

Jackson and Czarnecki [76] measured transition on six axisymmetric bodies at Mach 2.2 in the four-foot supersonic tunnel at Langley. The thin-skin heat-transfer models had 12 in. base diameters and were tested at zero AOA and adiabatic-wall conditions. Freestream unit Reynolds numbers ranged from $1.4–6.5 \times 10^6$/ft. Carborundum grit of 0.039 in. was used on most models to induce transition; this grit was said to be higher than the boundary-layer thickness, but was used due to the difficulty of tripping these flows. The smooth hemisphere remained laminar to the maximum Reynolds number, and a local $Re_\theta \simeq 700$. For the hemisphere with grit, the model was laminar for $Re < 2.7 \times 10^6$/ft. At $Re = 3.4 \times 10^6$/ft, the boundary layer began to be transitional just downstream of the roughness. However, the hemisphere with grit never became fully turbulent, even at the highest Reynolds number.

A smooth-hemisphere-cone model was laminar to the maximum Reynolds number. This model had a 4 in. nose radius and a 14.5 deg half-angle. However, when a strip of 0.025 to 0.028 in. grit was applied on the model face, the flow was transitional for the lower pressures and fully turbulent only for the higher pressures. To make the flow fully turbulent at the lower pressures, a second grit strip was applied in the region of adverse pressure gradient. This effect seems similar to that observed by Boudreau [77].

Model C had a blunted face; the geometry is not specified. The smooth-wall model C transitioned behind the shoulder at the maximum Reynolds number. Just as with the sphere cone, a first roughness strip only tripped the flow at the higher Reynolds number, and a second strip had to be added in the region of neutral-to-adverse pressure gradient to trip at the lower Reynolds number. Models D and E had different levels of blunting and similar performance.

These data appear useful for comparing with various roughness-induced-transition correlations. Although the Mach number is low, the blunt-body flow may be only weakly dependent on Mach number. The nonspherical shapes shed some light on the effect of variations in pressure gradient, but the geometries would probably have to be digitized from the drawings.

Hemisphere Cylinders at Mach 10.4 and 11.4

Dunavant and Stone [78] measured transition on hemisphere cylinders with a 6 in. diameter at unit Reynolds numbers of $0.23–2.2 \times 10^6$/ft. Four surface finishes were tested: a 4 μin. smooth surface, two surfaces with hemispherelike close-packed roughness arrays with heights of 0.025 and 0.050 in., and a random nodular roughened surface with an average height of 0.004 in. The latter was produced by spraying on molten copper. The measurements were made in the Langley 31-in. hypersonic tunnel during the original continuous-flow operation in the Mach-10 and Mach-11 nozzles. Transition was inferred from backface thermocouples on the thin-skin Inconel models. Although the study was focused on roughness-induced augmentation of stagnation-point heating, transition onset was apparently induced on the three roughest models at $s/D \simeq 0.2$ for $Re_D \simeq 0.3–1.0 \times 10^6$. The data appear worthy of reanalysis. Re_θ at transition onset was said to be 25–55 on these very rough models. No correlation of roughness-induced transition was attempted, although these data were among those included in Batt and Legner's [17] PANT-based correlation.

Hemispheres at Mach 2.01

Van Driest and Blumer [79,80] measured transition on 6.5-in.-diam hemispheres in the JPL 20 in. supersonic tunnel at Mach 2.01. Single rows of tripping spheres were placed on the hemisphere at various angles from 12.5 to 60 deg from the stagnation point. Spheres with diameters from 0.004 to 0.015 in. were used. Transition was determined by sublimation of azobenzene. The sudden widening of the vortex path behind the trips was taken as the onset of transition. Unfortunately, neither the journal paper nor the U.S. Air Force Office of Scientific Research report give any detailed tabulations or plots of the fundamental data.

Previously, Van Driest and Blumer [79,80] correlated roughness-induced transition on cones using $Re_{\delta^*}/(1 + 0.5(\gamma - 1)M_e^2)$ vs k/δ^*. Here, Re_{δ^*} is the Reynolds number based on edge conditions and displacement thickness, M_e is the edge Mach number, and δ^* is the displacement thickness. However, this gave a poor correlation to the new data on the hemispheres. Van Driest and Blumer therefore added a curvature term and obtained a curve fit to $Re_{\delta^*}/(1 + 0.5(\gamma - 1)M_e^2)$ vs $(k/\delta^*)/(1 + 700(k/D))$. Here, k is the roughness height and γ is the ratio of specific heats. The cubic curve fit is given in the paper, and Van Driest and Blumer argued that all of the data therefore follow essentially the same law. These data would be very valuable if sufficient detail can be found to permit reanalysis, but this seems doubtful. Terms can always be added to existing correlations when they fail to fit new data sets, but this process casts doubt on the generality of the correlation. What is needed is again a comprehensive attempt to find the prediction method that best correlates a wide variety of data. It is not clear if simple algebraic formulas will be sufficient for this purpose. Mechanism-based approaches may be required.

Hemispheres at Mach 5

Varwig [81] measured transition on a hemisphere with roughness in a Mach-5 shock tunnel at the Aerospace Corp. (see also [82]). Transition was inferred from heat-transfer measurements with thin-film gauges placed between the roughness elements, with the equivalent surface heat transfer inferred from other turbulent boundary-layer studies. Roughness was applied to the 4-in. hemisphere using glass beads. The smooth-wall hemisphere was laminar to a maximum Reynolds number of $Re_D = 2.9 \times 10^6$ at the stagnation temperature of about 900 K. For the 0.004-in.-diam beads, transition onset moved from 20 to 15 to 10 deg from the stagnation point as Re_D increased from 1.3 to 1.4 to 2.7 million. Although the rough-wall heat-transfer data are problematic due to the measurements at the base of the cavity between roughness elements, the transition data may be worthy of reanalysis. Varwig [81] also compared with measurements on a 7-in.-diam sphere by DiCristina in the Mach-5 tunnel at the Naval Ordnance Laboratory (NOL). Unfortunately, the DiCristina data do not appear to be available from any known archive.

Blunt Cones and Hemisphere at Mach 4

Coats [83] measured transition on a sphere cone, hemisphere, and compound sphere at Mach 4 and 8. The sphere cone had a 1.466 in. nose radius and a 10 deg half-angle. The hemisphere had a 2.932 in. radius, and the compound sphere had a 3.826 in. radius near the stagnation point. Transition was inferred from surface temperature gauges. The useful data was obtained at Mach 4 in tunnel A, as the instrumentation did not work well in tunnel B at Mach 8. Unfortunately, it appears that transition always occurred on the axial cylinders that followed the blunt forebodies, and so there are no data for transition on the blunt noses themselves.

Blunt Cones

Jackson [57] measured transition on blunt bodies in NOL tunnel 8 as part of the PANT program. Four of the models were sphere cones with nose radii of 0.75, 1.5, 2.5, and 3.5 in. and 8 deg half-angles. A biconic and a laminar-ablated shape were also tested. All of the models were grit-blasted to a surface roughness of 0.0035 in. The experiments were carried out at Mach 5 and unit Reynolds numbers ranging from 0.42 to 7.4 million per foot. Backface thermocouples were used on thin-skin models to infer heat transfer.

The noise in the tunnel freestream was measured under different conditions. The rms pressure fluctuations divided by the freestream dynamic pressure ranged from near 0.003 at the lowest Reynolds number to near 0.0007 at the highest Reynolds number. Detailed plots of the heat-transfer coefficient vs arc length are shown for all

runs. Transition moves forward as the unit Reynolds number and nose radius increases, but does not scale only with the nose-radius Reynolds number, perhaps because all models had the same surface roughness. The results are well documented and appear to be useful for evaluating transition-estimation methods.

Viking Aeroshell at Mach 8

Creel [84] measured heating to the blunt-sphere-cone Viking aeroshell in the NASA Langley variable-density tunnel at Mach 8. The model included isolated protuberances and cavities expected to be characteristic of the flight vehicle. Aeroheating was measured using fusible temperature paint. The model was 11.68 cm in diameter and was tested at freestream unit Reynolds numbers of $3.7–17 \times 10^6$/m. Interference heating was measured aft of the isolated surface flaws. Because there was no marked dependence of the nondimensional heating on the Reynolds number, it may be that all of the measurements reflect interference heating that is basically laminar. This is not too surprising, because $Re_D < 2 \times 10^6$. A reanalysis of the protuberance wakes would be of interest.

Hemisphere at Mach 6

Laderman [85] measured transition on 14-in.-diam porous and roughened hemispheres in tunnel B at $Re_D = 2.8–6.2 \times 10^6$. Pitot tubes and hot wires were used to obtain profiles of the flow at 40 deg from the stagnation point. Four roughness overlays were tested: these had effective peak-to-valley roughness heights of 1.44, 1.70, 2.36, and 4.77 mil. The model was internally cooled with liquid nitrogen. The flow was completely laminar with the smallest roughness under adiabatic conditions. Transition compared favorably with the PANT correlation (see also [86] for similar data with blowing effects from a porous hemisphere). These data should be reanalyzed with modern computational methods, but the details are available only in reports with limited distribution.

Blunt Bicones at Mach 15–20

Richards and DiCristina [87] measured transition on blunt bicones in the von Karman Institute (VKI) hot-shot tunnel at Mach 15–20. The Reynolds numbers based on freestream conditions and model base diameter were $1.2–5 \times 10^6$. The model nose radius was 0.75 in. and the base diameter was 7.00 in. The forecone had a 50 deg half-angle followed by an 8 deg half-angle aft cone. Transition was inferred from flush calorimeters. Transition Reynolds numbers based on momentum thickness Re_θ ranged from 250–400 on smooth models and decreased 25% when 4 mil of evenly distributed roughness was added. Unfortunately, the data are fairly sparse and are not presented in much detail, and so unless a more detailed report can be found, a reanalysis does not appear to be warranted.

Hemispheres in the Ballistic Range

Reda [88,89] made several measurements of transition on various nosetip materials using hemispheres in the ballistic range. Reda [89] compared the performance of ATJ-S, CMT, Graphnol, 223 C/C, and FWPF materials. All flights were carried out at 16.0 kft/s into air at 540°R. The surface microroughness of the laminar preablated specimens was measured using microscopy. The peak-to-valley heights for the bulk graphites varied from 0.168 mil for Graphnol to 0.383 mil for CMT to 0.638 mil for ATJ-S. The peak-to-valley heights for the woven materials were 0.422 mil for 223 C/C and 0.271 mil for FWPF. Nose radii varied from 0.4 to 1.25 in. Transition was detected using electro-optical pyrometry images.

The smoother materials exhibit transition farther downstream or at higher Reynolds numbers, as shown in Fig. 8. Here, S is the arc length along the hemisphere from the nose, R_N is the nose radius, and P_∞ is the freestream static pressure. The solid lines enclose regions in which the original plot shows a solid area over which the data were distributed. Correlations of these data are shown in [15]. The best fit was achieved with a correlation based on the roughness Reynolds number Re_k.

Hemispheres with Small Craters at Mach 5

Todisco et al. [90] measured transition on hemispherical nosetips in tunnel 8 at the Naval Surface Warfare Center. The models included small craters that simulated the effect of particle impacts. The nosetip radii were 2.5 and 1.0 in., and the wall-to-stagnation-temperature ratio was 0.3. Unit Reynolds numbers varied from $1–20 \times 10^6$/ft, and transition was inferred from 75 backface thermocouples. The models were polished to 2–4 μin. and then the craters were machined using custom tool bits. Both single and multiple craters were tested.

At low Reynolds numbers, the boundary layer remained laminar behind the crater. At higher Reynolds numbers, the boundary layer appeared to trip behind the crater but then relaminarized downstream; this behavior was termed *crater transition*. At yet higher Reynolds numbers, the boundary layer tripped and remained turbulent. For conical craters of depth $k = 0.020$ in., Re_k varied from about 1000 to 8000 for single-crater tripping, with the value and the variation in the value both increasing with the angle from the stagnation point. Todisco et al. [90] noted that the values are larger than those predicted using Van Driest and Blumer's [79] correlation. Craters with a greater diameter-to-depth ratio were tripped at Re_k values that were 2–3 times lower than smaller craters. Deeper craters tripped at larger Re_k, in accordance with Van Driest and Blumer's correlation, which attributes the effect to variations in k/R_N, where R_N is the nose radius. The PANT correlation is also used for comparison.

Because the basic data are not given, reanalysis is not possible with public-domain information. This report by Todisco et al. [90] provides useful data. However, it would be better to have more details on how the experiments were conducted, so that other correlations can be compared using modern computational techniques.

Hemispheres in the Ballistic Range

Wassel et al. [91] measured transition on simulated nosetips using the rails in track G at AEDC. The models were made from tungsten, ATJ-S, 994-2 graphite, 223 carbon-carbon, and FWPF. The tungsten models were built with nose radii of 0.25 and 0.40 in. and surface roughness ranging from 1.7 mil to less than 10 μin.. The graphitic models had 3/8 in. nose radii and were preablated laminar in a plasma arc. Optical pyrometry was used to image the transition front in flight. Wassel's Table 1 lists 11 shots at speeds all near 16 kft/s, static range temperatures near 540°R, and static range pressures ranging from 70 to 570 torr.

The smooth tungsten hemisphere was laminar at a range pressure of 570 torr and $Re_D = 2.9 \times 10^6$. The heating rate at the stagnation point was about 17×10^7 W/m^2. Wassel et al's [91] results for transition location were not in good agreement with the usual nosetip-roughness correlations, for reasons that are not clear to this

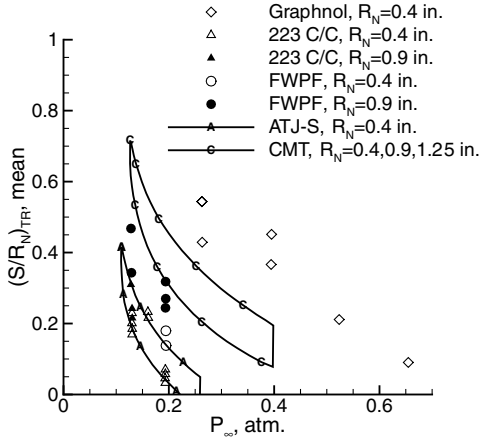

Fig. 8 Transition front location vs freestream static pressure for ballistic-range measurements on hemispheres (redrawn from [89], Fig. 8).

author. The PANT correlations given by Wassel et al. include corrections for surface blowing effects.

Spheres at Mach 5

Schöler [92] measured boundary-layer transition on the front portion of spheres that were sting-mounted in the Mach-5 Ludwieg tube in Göttingen. Transition was measured using liquid crystals. The brief summary paper shows laminar flow at $Re_D = 2 \times 10^6$, turbulent wedges behind roughness at 3–3.6 $\times 10^6$, mostly turbulent flow at 4×10^6, and fully turbulent flow at 4.5×10^6. The roughness due to the liquid crystals is given as 0.01 to 0.02 mm, but the sphere diameter is not given in this brief summary report. The data might be very useful for reanalysis if more detail can be obtained, but none has so far been located.

Hemisphere at Mach 12 to 16

Many measurements of aeroheating and transition have been made in the well-established group of large shock tunnels at Calspan —University at Buffalo Research Center. Many papers and reports have been published, but it can still be difficult to find specific details for configurations of interest.

Holden [93] was primarily concerned with augmented turbulent heating at the stagnation point of blunt bodies. However, he also reports shock-tunnel measurements on hemispheres with a 12 in. diameter. Figure 9 in the reference shows transition onset at about 3 in. from the stagnation point for a freestream Reynolds number of 11 million per foot at Mach 11. Unfortunately, the temperatures are not given. For the same hemisphere at the same Mach number at a Reynolds number of 4 million per foot, the flow is completely laminar. Trip rings of 0.010 and 0.020 in. heights were also used at different locations. However, the data are not complete enough to permit reanalysis.

Holden and Rodriguez [94] were primarily concerned with shock/shock interactions near blunt noses, but included measurements of smooth and transpiration-cooled hemispheres in the Calspan Advanced Technology Center 48-in. shock tunnel. Heat-transfer measurements were made with thin-film gauges. Freestream unit Reynolds numbers ranged from 4×10^4/ft to 1.6×10^6/ft and the large models had a 6-in. nose radius, leading to $Re_D \simeq 0.04$–1.6×10^6, even at the high freestream Mach numbers of 12 to 16. Holden's [93] Fig. 14 shows that the smooth hemispheres were laminar to 4.3×10^5/ft at Mach 16.2. Figure 16 in [94] shows an increase in heating on the rough transpiration-cooled hemispheres at about 40 deg from the stagnation point, at both 3.2×10^5/ft and 1.5×10^6/ft., with the coolant flow off. Unfortunately, there are no clear data for transition (as opposed to slot-disturbance-augmented laminar heating), and the roughness of the slotted transpiration-cooled nose is not clear. Reference [94] is suggestive of the capabilities of the large shock tunnels, but in itself does not seem to contain useful data for comparison with improved methods of estimating transition.

Transition on Blunt Sphere Cones at Mach 9

Zanchetta and Hillier [95] measured transition on a blunt sphere cone with a 5 deg half-angle in the Imperial College gun tunnel at Mach 9 . Thin-film heat-transfer gauges were used to infer transition. Zanchetta and Hillier observed that for small-nose-radius Reynolds numbers of 3×10^5 or less, increased nose radii delayed transition on the cone. For larger-nose-radius Reynolds numbers, transition became sensitive to small surface imperfections, and small roughness elements in the subsonic region on the nose caused transition to jump forward to the sphere-cone junction. These observations are similar to those reported by Stetson [72], who suggested a different scaling (see also the discussion in [13]). However, few details are presented in this short conference paper.

More detail is available in [96]. Twelve nose radii were tested at three unit Reynolds numbers. The nose radii varied from sharp to 25 mm, and the freestream Reynolds number was 7.5, 12.6, or 47.4 million per meter, with stagnation temperatures near 1100 K. The diameter of the Mach-9 core flow is about 280 mm and the duration of steady flow is about 4–7 ms. In most cases, it was still difficult to determine the locations of the beginning and end of transition, because all of the sensors seemed to be in between. At 47.4 million per foot, the end of transition appeared to be near 0.48 m for the 2 mm nose radius and near 0.62 m for the 3 mm nose radius. At 12.6 million per foot, the beginning of transition was near 0.36 m for the 2 mm nose and 0.62 m for the 3 mm nose; the end of transition was near 0.6 m for the 2 mm nose. The sharp cone was turbulent for the two higher Reynolds numbers. The length of the transitional zone seemed to decrease dramatically when the nose bluntness increased into the region in which roughness on the nose seemed to dominate transition. However, there is considerable uncertainty regarding the appropriate method of interpreting the data.

Recent VKI Measurements of Roughness-Induced Transition

Carbonaro et al. [97] made several measurements of roughness-induced transition at hypersonic speeds on models at the von Karman Institute tunnels in Belgium (see, for example, [98,99]). However, up to 1996, the measurements were made on sharp cones and flat plates and were compared with Bertin et al.'s [100] shuttle-based approach. Carbonaro et al. ([97], page 2A-13) were not able to trigger transition using roughness elements on the blunt face of a hemispherical model, probably because the Reynolds numbers in the VKI tunnels are too small.

Charbonnier et al. [101] reported additional measurements on blunt bodies at Mach 6, in support of tripping efforts for the Atmospheric Reentry Demonstrator, a very blunt Apollo-like shape. The measurements were performed in a 6-in. Mach-6 open-jet tunnel at freestream Reynolds numbers of 8–20 $\times 10^6$/m. Hemisphere cylinders and blunt sphere cones were studied: all had a nose radius of 20 mm. Distributed roughness was applied by knurling, and isolated roughness was also tested in the form of spheres. Large isolated roughness heights k were needed to trip the flow, with k/δ^* of 1–5 being correlated against $Re_e(x_{\rm tr} - x_{\rm sphere})/M_e^2$. Here, $x_{\rm sphere}$ appears to be the arc length from the nose to the location of the tripping sphere, but the symbols in [101] are not all defined. Distributed roughness was more effective at tripping, but was only successful on the cylindrical portion of the hemisphere cylinder. The data are limited and do not appear successful in tripping on the hemisphere itself, probably because the Reynolds numbers are too low ($Re_D \simeq 0.32$–0.80×10^6).

Paris et al. [102] described measurements on the Expert reentry geometry in the H3 and Longshot tunnels at VKI. The Expert vehicle is a very blunt pyramidal shape; the geometry is not specified. It appears that the shape, which is roughly 50% blunt, was split in two lengthwise to enable starting a larger model. The model was about 24 cm long, the height across the half-base was about 16 or 18 cm, and the roughness elements were placed 44 or 118 mm from the nose. Measurements were made with an infrared camera in the H3 tunnel at Mach 6 using isolated roughness with six heights ranging from 0.1 to 0.98 mm. Transition was inferred from the infrared images, in a way that is not specified. The results were then compared with the PANT correlation, which was fairly successful for the Mach-6 data. A shuttle-type correlation was not successful. Data were obtained in the Longshot tunnel at Mach 15 and unit Reynolds numbers to 7.5 million per meter, but these data do not agree with the PANT correlation. The few details given are insufficient to enable reanalysis.

Seventy-Degree Sphere Cone at Mach 6

Horvath et al. [103] measured the near-wake flow on a blunt planetary-probe shape in the 20-in. Mach-6 tunnel at Langley. The nose radius was 1.5 in. and the diameter of the model was 6 in. The model was fixed at zero AOA and tested at $Re_D = 0.5$–4.0×10^6. For some of the tests, aluminum oxide grit of about 0.015 in. in diameter was dispersed on the forebody stagnation region. The ratio of roughness height to displacement thickness is stated to vary from about 3 near the stagnation point to about 1.2 near the end of the grit at about 90% of the radius, but the Reynolds number at which this was

estimated is not given. Heat-transfer distributions were inferred from coaxial thermocouples and thin films.

For the two higher Reynolds numbers of 2 and 4 million, the forebody boundary layer transitioned to turbulence. For the lower Reynolds number of 0.5 million, the boundary layer did not transition, and the heating returned to laminar levels as the flow expanded around the model shoulder. Although this paper is focused on the wake flow, the measurements on the blunt face are suggestive of the conditions necessary for obtaining transition and might be worth reanalyzing.

Genesis Sample-Return Capsule

Transition on the Genesis sample-return capsule was measured in a Mach-6 wind tunnel by Cheatwood et al. [104]; this work was inadvertently omitted from [11]. Cheatwood et al. [104] measured transition induced by surface cavities in the 20-in. Mach-6 tunnel at Langley. Four models with diameters of 3, 4, 5, and 6 in. were used, but it appears that only the 6 in. models were used for the transition measurements. The circular cavities were placed at 40 and 70% of the distance from the stagnation point to the rim. At zero angle of attack, the smallest cavity did not trip the flow, but the larger cavities did. A preliminary correlation of the transition location was plotted using Re_θ vs w/δ, where w is the cavity diameter and δ is the boundary-layer thickness.

The sample-return capsule reentered the atmosphere on 8 September 2004. Although the parachute failed, much of the heat shield was recovered intact [105]. It appears that transition occurred in a wedge downstream of the penetration, leaving a discolored region on the heat shield. The spreading angle in the wake is about 4–5 deg, a value similar to that observed by Van Driest and Blumer [79] behind spherical trips on a hemisphere at Mach 2 [80]. Navier–Stokes computations show that transition increases the heating rate by a factor of more than 2 [105].

Unfortunately, it appears that the in-flight roughness due to the molybdenum penetration is not known. If the in-flight roughness can be inferred using postflight measurements of the recovered hardware, it might be useful to revisit this issue so that the flight data can be used to help understand blunt-body transition induced by roughness and cavities.

Mars Science Laboratory

Transition on the Mars Science Laboratory (MSL) [106] was reviewed in [11]. Since the preparation of that paper, [107–109] became available. Edquist et al. [108] provided computations of the laminar and turbulent aeroheating; the vehicle was designed for turbulent heating to the blunt face and thrust-plume interference heating to the afterbody. The blunt-face boundary layer is expected to become turbulent before peak heating. Transition to turbulence increases the computed smooth-wall nonablating peak heating rate by a factor of 2.5.

Hollis and Collier [109] reported measurements on MSL in AEDC tunnel 9 at high Reynolds numbers. The measurements were made on 6-in.-diam solid-metal models in perfect-gas nitrogen at Mach 8 and 10 for unit Reynolds numbers from 1 to 49 million per foot. Heating and transition were inferred from flush-mounted thermocouples. Because the experiments were focused on turbulent heating, the transition data were not analyzed in detail.

Transition appeared to depend on Mach number, because at Mach 10 it began near 15 million per foot, whereas at Mach 8 it began near 8 million per foot. Because the noise level in tunnel 9 does not change much between these two Mach numbers, the source of this dependence is unknown [110]. The surface finish of the model is not given; it seems possible that particulate impact increased the roughness during the initial runs at Mach 10, but no evidence of such an effect is evident in the repeated runs. It is also possible that the apparent difference is simply an artifact of the large changes in unit Reynolds number between runs. However, Figs. 21, 22, 25, and 26 in the reference suggest a Mach number effect in addition to the Reynolds number effect.

The flow was thought to be transitional if the heating levels were significantly above laminar computations, yet well below turbulent computations. Without measurements of the fluctuations in the boundary layer, this inference cannot be confirmed.

Hollis and Collier [109] also reported measurements in the 20-in. Mach-6 tunnel at Langley using surface thermocouples in a metal model instead of the usual phosphor-coated ceramic model. Transition occurred much later on the metal model, suggesting a significant impact of the surface roughness of the phosphor coating. It would be very interesting to see an analysis of transition using the computations and measurements in these two tunnels.

Offset Hemisphere Cylinder at Mach 9

Schrijer et al. [111] measured on a hemisphere cylinder in a Mach-9 Ludwieg-tube wind tunnel using infrared thermography. The freestream unit Reynolds number varied from $4–14 \times 10^6$/m. The hemisphere had a 5 cm radius and was offset from the cylindrical afterbody by a height h, which ranged from -3.2 to 3.2 mm. Distributed roughness and tripping wires were also applied to the model nose. The heat transfer increased with roughness height, although it is not clear from the short paper that turbulent heating was achieved, as opposed to disturbed laminar heating. The results were correlated using PANT, Re_k, and a shuttle-type approach. The grit roughness correlates well, but the step roughness does not. Few details are shown, and so it would be impossible to reanalyze the data.

Ballistic-Range Measurements on Hemispheres

Reda et al.'s [112] work in the NOL and AEDC ballistic ranges was later continued at NASA Ames. The Ames range and a general review of range measurements of roughness-induced transition is reported in [112]. Additional measurements on POCO graphite are reported in [113]. Additional transition data were measured for both laminar-ablated and bead-blasted POCO graphite hemispheres. The bead-blasted models had nose radii of 0.375 and were flown near 12 kft/s at range pressures from 0.58 to 0.75 atm. The roughness was about 0.57 mil. The laminar-ablated models had nose radii of 0.75 in. and were flown near 14 kft/s at range pressures from 0.25 to 0.38 atm. Heating rates were imaged using an intensified charge-coupled device camera. Transition occurred on the noses and was correlated with Re_k, along with previous data. For values of

$$0.5 \le \frac{\rho_k u_k \bar{k}}{\rho_e u_e \theta} \le 2.5$$

transition was correlated at $\rho_k u_k \bar{k}/\mu_w = 250$. Here, ρ_k and u_k are density and velocity in the undisturbed boundary layer at the roughness height k, ρ_e and u_e are density and velocity at the boundary-layer edge, μ_w is the viscosity at the wall, $\bar{k}$ is the average roughness height, and θ is the momentum thickness. For

$$\frac{\rho_k u_k \bar{k}}{\rho_e u_e \theta} < 0.5$$

the flow was thought to be in the smooth-wall limit, where $\rho_e u_e \theta/\mu_w = 500$ at transition. This smooth-wall limit is not generally valid, for much larger values have sometimes been measured [12,17], but it may be useful for preliminary design. For

$$\frac{\rho_k u_k \bar{k}}{\rho_e u_e \theta} > 2.5$$

the flow was thought to be in a large-roughness limit at low Reynolds numbers, for which transition was expected at $\rho_e u_e \theta/\mu_w = 100$. It would be interesting to see if the proposed large-roughness limit was consistently valid for measurements at other conditions and in other facilities.

Supersonic Measurements on Orion

Murphy et al. [114] measured aerodynamic forces on the Orion vehicle in the Unitary Plan Wind Tunnel at NASA Langley. The

3.03% model was 6 in. in diameter and was tested mostly at a unit Reynolds number of 3×10^6/ft for Mach numbers from 1.6 to 4.0. The angle of attack varied from 10 to 30 deg. Transition was inferred from qualitative images of heat transfer obtained using temperature-sensitive paint and an infrared camera.

For $Re_D = 1.5 \times 10^6$ at Mach 1.6, 2.0, and 2.5, the smooth model appeared to be laminar. At $Re_D = 2.5$–3.5×10^6 and Mach 1.6, the flow was transitional, with streaks of turbulence emanating from probable roughness in the nominally smooth wall (the surface finish was not given). Distributed roughness was applied in a narrow strip around the stagnation point, with roughness height varying from 0.005 to 0.012 in. The roughness height was determined using a simple analysis based on [115]. The trips were successful in generating a turbulent flow. The blunt face of the smooth model became pitted during tunnel operation, due to the impact of particulate; these pits were also able to trip the flow [[114], Fig. 16].

Dynamic stability is an issue for Orion development; it is very difficult to compute, due to the sensitivity of the moment coefficients to small errors [116]. Although [116] did not discuss the effect of transition on these moments, [117] showed that transition had a large effect on these moments for the Mercury spacecraft [11]. However, [114] showed that transition has little effect on the Orion moments at supersonic speeds, perhaps because Orion does not have the extended afterbody that Mercury and Gemini did.

Conclusions

Laminar-turbulent transition on blunt geometries occurs when the Reynolds number is high enough, given a geometry, surface roughness, Mach number, stagnation enthalpy, wall temperature, tunnel noise level, angle of attack, and so on. For nominally smooth models, it appears that Reynolds numbers based on freestream conditions and diameter must be several million or more. For models with roughness typical of flight, a wide range of existing data suggest that Reynolds numbers must still be of the order of a million or more. When roughness increases, the transition Reynolds number falls. At high Reynolds numbers, transition is sensitive to roughness that often appears small; a general quantitative definition of high and small remains to be determined. Low but significant levels of roughness are often introduced inadvertently by freestream particulate. Furthermore, it is difficult to reach sufficiently high Reynolds numbers in most facilities, because blunt models must be relatively small to permit successful starting of the tunnel. Thus, experimental data for blunt-body transition are rare and expensive to obtain. Accurate and reliable prediction of roughness-induced transition on blunt bodies remains a topic for future research.

Considerable data exist for the Apollo vehicle using various configurations of protuberances and trips. Given the cost of acquiring more data of this type, it may be cost-effective to reanalyze these data to determine the conditions under which the roughness induced transition. Much of the data are tabulated and plotted in detail, although the signs and symbols are not always defined well enough to make a reanalysis straightforward, and the necessary computational comparisons for a blunt three-dimensional vehicle at angle of attack are still not easy to obtain.

Even more data exist for other blunt geometries, primarily the hemispherical-type shapes used for the nosetips of military reentry vehicles. Many measurements were made on these shapes at great expense during the Cold War. Although these data also suffer from various limitations, it again appears cost-effective to reanalyze it in a systematic way using modern computational methods.

A number of different algebraic formulas have been developed in attempts to correlate roughness-induced transition. Because these formulas are in common use for engineering design, it would be interesting to see if any of them provide a good fit to a wide variety of experimental data. Unfortunately, there has been no such effort to perform a systematic evaluation for a wide variety of these correlations. Such an effort is apparently considered as too applied for basic research funded at NASA or in academia, although it has always been considered as too fundamental to be carried out as part of a particular vehicle design. The data summarized in the present review should be used to carry out such an evaluation of the most promising methods for estimating roughness-induced transition. A comprehensive evaluation of this type would determine the conditions under which the classical algebraic formulas correlate the data reasonably well. Such an evaluation may find that more sophisticated mechanism-based methods are needed to achieve satisfactory agreement for a wide range of data.

Acknowledgments

Much of the work of developing this review was funded by the Northrop Grumman Corporation as preparation for the development of the Orion vehicle. The author's research has been funded by the U.S. Air Force Office of Scientific Research, Sandia National Laboratory, NASA Johnson Space Center, NASA Langley Research Center, and NASA's Constellation University Institutes Project.

References

[1] Saric, W. S., "Görtler Vortices," *Annual Review of Fluid Mechanics*, Vol. 26, 1994, pp. 379–409.

[2] Mack, L. M., "Boundary Layer Linear Stability Theory," *Special Course on Stability and Transition of Laminar Flow*, AGARD, Rept. 709, Neuilly-sur-Seine, France, Mar. 1984, pp. 1–81.

[3] Saric, W. S., Reed, H. L., and White, E. B., "Stability and Transition of Three-Dimensional Boundary Layers," *Annual Review of Fluid Mechanics*, Vol. 35, 2003, pp. 413–440. doi:10.1146/annurev.fluid.35.101101.161045

[4] Arnal, D., and Casalis, G., "Laminar-Turbulent Transition Prediction in Three-Dimensional Flows," *Progress in Aerospace Sciences*, Vol. 36, No. 2, Feb. 2000, pp. 173–191. doi:10.1016/S0376-0421(00)00002-6

[5] Reshotko, Eli., and Tumin, Anatoli., "Role of Transient Growth in Roughness-Induced Transition," *AIAA Journal*, Vol. 42, No. 4, Apr. 2004, pp. 766–770. doi:10.2514/1.9558

[6] Abbott, Ira H., "Some Factors Contributing to Scale Effect at Supersonic Speeds," AGARD, Rept. AG4/M4, Neuilly-sur-Seine, France, Sept. 1953.

[7] Schneider, S. P., "Effects of High-Speed Tunnel Noise on Laminar-Turbulent Transition," *Journal of Spacecraft and Rockets*, Vol. 38, No. 3, May–June 2001, pp. 323–333. doi:10.2514/2.3705

[8] Borg, Matthew P., Schneider, S. P., and Juliano, T. J., "Effect of Freestream Noise on Roughness-Induced Transition for the X-51A Forebody," AIAA Paper 2008-0592, Jan. 2008.

[9] Schneider, S. P., "Development of Hypersonic Quiet Tunnels," *Journal of Spacecraft and Rockets*, Vol. 45, No. 4, July–Aug. 2008, pp. 641–664. doi:10.2514/1.34489

[10] Casper, K. M., Wheaton, B. M., Johnson, H. B., and Schneider, S. P., "Effect of Freestream Noise on Roughness-Induced Transition at Mach 6," AIAA Paper 2008-4291, June 2008.

[11] Schneider, S. P., "Laminar-Turbulent Transition on Reentry Capsules and Planetary Probes," *Journal of Spacecraft and Rockets*, Vol. 43, No. 6, Nov.–Dec. 2006, pp. 1153–1173; also Erratum Vol. 44, No. 2, Mar.–Apr. 2007, pp. 464–484. doi:10.2514/1.30727

[12] Schneider, S. P., "Flight Data for Boundary-layer Transition at Hypersonic and Supersonic Speeds," *Journal of Spacecraft and Rockets*, Vol. 36, No. 1, 1999, pp. 8–20. doi:10.2514/2.3428

[13] Schneider, S. P., "Hypersonic Laminar-Turbulent Transition on Circular Cones and Scramjet Forebodies," *Progress in Aerospace Sciences*, Vol. 40, No. 1–2, 2004, pp. 1–50. doi:10.1016/j.paerosci.2003.11.001

[14] Schneider, S. P., "Effects of Roughness on Hypersonic Boundary-Layer Transition," *Journal of Spacecraft and Rockets*, Vol. 45, No. 2, Mar.–Apr. 2008, pp. 193–209. doi:10.2514/1.29713

[15] Reda, D. C., "Correlation of Nosetip Boundary-layer Transition Data Measured in Ballistics-Range Experiments," *AIAA Journal*, Vol. 19, No. 3, Mar. 1981, pp. 329–339. doi:10.2514/3.50952

[16] Reda, D. C., "Review and Synthesis of Roughness-Dominated Transition Correlations for Reentry Applications," *Journal of Spacecraft and Rockets*, Vol. 39, No. 2, Mar.–Apr. 2002, pp. 161–167. doi:10.2514/2.3803

[17] Batt, R. G., and Legner, H. H., "A Review of Roughness-Induced Nosetip Transition," *AIAA Journal*, Vol. 21, No. 1, Jan. 1983, pp. 7–22; also AIAA Paper 81-1223, June 1981.
[18] Berry, S., and Horvath, T., "Discrete Roughness Transition for Hypersonic Flight Vehicles," AIAA Paper 2007-0307, Jan. 2007.
[19] Schneider, S. P., "Hypersonic Boundary-Layer Transition on Blunt Bodies with Roughness," AIAA Paper 2008-0501, Jan. 2008.
[20] Schneider, S. P., "Hypersonic Boundary-Layer Transition with Ablation and Blowing," AIAA Paper 2008-3730, June 2008.
[21] Amar, A. J., Horvath, T. J., Hollis, B. R., Berger, K. T., Berry, S. A., and Calvert, N., "Protuberance Boundary Layer Transition for Project Orion Crew Entry Vehicle," AIAA, Paper 2008-1227, Jan. 2008.
[22] Schneider, S. P., "Laminar-Turbulent Transition on Reentry Capsules and Planetary Probes," AIAA Paper 2005-4763, June 2005.
[23] "Experimental Heat Transfer and Pressure Distributions over Entry Configurations of 0.02-Scale Apollo Models H-1 and PS-1 and Hemisphere-Cylinders at Mach Number of 10," NASA CR 117543, Jan. 1963; also North American Aviation, Inc., Space and Information Div., Rept. SID-63-623, Downey, CA, 1963.
[24] Fox, G. L., and Marvin, J. G., "An Investigation of the Apollo Afterbody Pressure and Heat Transfer at High Enthalpy," NASA TM-X-1197, Mar. 1966.
[25] Miller, C. G., III, and Lawing, P. L., "Experimental Investigation of Flow Characteristics of the Apollo Reentry Configuration at a Mach Number of 20 in Nitrogen," NASA TM-X-1258, July 1966.
[26] Lee, G., and Sundell, R. E., "Heat-Transfer and Pressure Distributions on Apollo Models at Mach 13.8 in an Arc-Heated Wind Tunnel," NASA TM-X-1069, Feb. 1965.
[27] Lee, G., and Sundell, R. E., "Apollo Afterbody Heat Transfer and Pressure with and Without Ablation at Mach 5.8 to 8.3," NASA TN-D-3620, Sept. 1966.
[28] Kemp, J. H., Jr., "Telemetry Measurements of Afterbody Pressures on Free-Flying Models of the Apollo Capsule at Mach Numbers from 10 to 21 in Helium and 14 in Air," NASA TM-X-1154, Oct. 1965.
[29] Akin, C. M., "Experimental Comparison of Apollo Afterbody Heating in Air and Carbon Dioxide," NASA TM-X-1204, Jan. 1966.
[30] Gorowitz, H., "NAA Shock Tunnel Tests /St-4/ of Apollo Command Modules H-6 and PS-6," CR-117702, NASA, Aug. 1962; also North American Aviation, Inc., Space and Information Div., Rept. SID-62-1072, Downey, CA, 1962.
[31] DeRose, C. E., "Trim Attitude, Lift and Drag of the Apollo Command Module with Offset Center-of-Gravity Positions at Mach Numbers to 29," NASA TN-D-5276, June 1969.
[32] Sammonds, R. I., "Forces and Moments on an Apollo Model in Air at Mach Numbers to 35 and Effects of Changing Face and Corner Radii," NASA TM-X-1086, Apr. 1965.
[33] Lawrence, W. R., and Norman, W. S., "Free-Flight Range Tests of the Apollo Command Module," Arnold Engineering Development Center, TR 68-224, Tullahoma, TN, Jan. 1969.
[34] Bertin, J. J., "The Effect of Protuberances, Cavities, and Angle of Attack on the Wind-Tunnel Pressure and Heat-Transfer Distribution for the Apollo Command Module," NASA TM-X-1243, Oct. 1966.
[35] Biss, W. J., and Emerson, D. X., "Experimental Heat Transfer Distributions over Launch and Entry Configurations of an 0.045 Scale Apollo Model /H-2/ at Mach Numbers of 8 and 10," NASA CR-117538, Sept. 1962; also North American Aviation, Inc., Space and Information Div., Rept. SID-62-993-VOL-1, Downey, CA, 1962.
[36] Emerson, R. X., "Experimental Heat Transfer Distributions over the 0.090-Scale Apollo Command Module /H-11/ with Protuberances at Mach Number 10," NASA CR-117540, Nov. 1964.
[37] Emerson, R. X., "Heat Transfer Tests of the 0.090-Scale Apollo Entry Configuration /H-11/ in the AEDC-VKF Hypersonic Tunnel C," NASA CR-154529, June 1964.
[38] Fromm, E. H., "Apollo Model /H-1/ Wind Tunnel Test /JPL 21-102/," Vol. 1, NASA CR-117670, June 1962.
[39] Fromm, E. H., "Apollo Model /H-1/ Wind Tunnel Test /JPL 21-102/," Vol. 2, NASA CR-116724, June 1962.
[40] Lees, L., "Laminar Heat Transfer over Blunt-Nosed Bodies at Hypersonic Flight Speeds," *Jet Propulsion*, Vol. 26, pp. 259–269, Apr. 1956.
[41] Jones, R. A., and Hunt, J. L., "Effects of Cavities, Protuberances, and Reaction-Control Jets on Heat Transfer to the Apollo Command Module," NASA TM-X-1063, Mar. 1965.
[42] Hunt, J. L., and Jones, R. A., "Effects of Several Ramp-Fairing, Umbilical, and Pad Configurations on Aerodynamics Heating to Apollo Command Module at Mach 8," NASA TM-X-1640, Sept. 1968.
[43] Jones, R. A., and Hunt, J. L., "Recent Experimental Studies on Heat Transfer to Apollo Command Module," *Conference on Langley Research Related to the Apollo Mission*, NASA, Jan. 1965, pp. 9–18.
[44] "Apollo Wind Tunnel Model Nomenclature," NASA, CR-153876, July 1964; also North American Aviation, Inc., Space and Information Div., Rept. SID-63-44-R-3, Down, CA, 1963.
[45] "Apollo Wind Tunnel Program Report," NASA CR-156432, Feb. 1963; also North American Aviation, Inc., Space and Information Div., Rept. SID-62-170-4, Downey, CA, 1962.
[46] "Apollo Wind Tunnel Program Report," NASA CR-156445, July 1963; also North American Aviation, Inc., Space and Information Div., Rept. SID-62-170-5, Downey, CA, 1962.
[47] Udvardy, G. A., "Data Report for Experimental Heat Transfer Distributions over Launch and Entry Configurations on the 0.045-Scale Apollo Model /H-2/ with the Addition of Strakes at a Mach Number of 10," NASA CR-117230, Feb. 1964; also North American Aviation, Inc., Space and Information Div., Rept. SID-63-1135-VOL-1, Downey, CA, 1963.
[48] "Experimental Heat Transfer Distributions over Launch and Entry Configurations on the 0.045-Scale Apollo Model /H-2/ with the Addition of Strakes at a Mach Number of 10," Vol. 3, NASA CR-116644, Feb. 1964; also North American Aviation, Inc., Space and Information Div., Rept. SID-63-1135-VOL-3, Downey, CA, 1963.
[49] "Experimental Heat Transfer Distributions over Launch And Entry Configurations on the 0.045-Scale Apollo Model /H-2/ with the Addition of Strakes at a Mach Number of 10," Vol. 6, NASA CR-116647, Feb. 1964; also North American Aviation, Inc., Space and Information Div., Rept. SID-63-1135-VOL-6, Downey, CA, 1963.
[50] Biss, W. J., and Emerson, D. X., "Experimental Heat Transfer Distributions over Launch and Entry Configurations of an 0.045 Scale Apollo Model /H-2/ at Mach Numbers of 8 and 10," Vol. 3, NASA CR-117551, Sept. 1962; also North American Aviation, Inc., Space and Information Div., Rept. SID-62-993-VOL-3-APP-A, Downey, CA, 1962.
[51] Biss, W. J., and Emerson, D. X., "Experimental Heat Transfer Distributions over Launch and Entry Configurations of an 0.045 Scale Apollo Model /H-2/ at Mach Numbers of 8 and 10," Vol. 6, NASA CR-117300, Sept. 1962; also North American Aviation, Inc., Space and Information Div., Rept. SID-62-993-VOL-6-APP-B, Downey, CA, 1962.
[52] Biss, W. J., and Emerson, D. X., "Experimental Heat Transfer Distributions over Launch and Entry Configurations of an 0.045 Scale Apollo Model /H-2/ at Mach Numbers of 8 and 10," Vol. 2, NASA CR-117542, Sept. 1962; also North American Aviation, Inc., Space and Information Div., Rept. SID-62-993-VOL-2-APP-A, Downey, CA, 1962.
[53] Biss, W. J., and Emerson, D. X., "Experimental Heat Transfer Distributions over Launch and Entry Configurations of an 0.045 Scale Apollo Model /H-2/ at Mach Numbers of 8 and 10," Vol. 4, NASA CR-117555, Sept. 1962; also North American Aviation, Inc., Space and Information Div., Rept. SID-62-993-VOL-4-APP-B, Downey, CA, 1962.
[54] Biss, W. J., and Emerson, D. X., "Experimental Heat Transfer Distributions over Launch and Entry Configurations of an 0.045 Scale Apollo Model /H-2/ at Mach Numbers of 8 and 10," Vol 5, NASA CR-117297, Sept. 1962; also North American Aviation, Inc., Space and Information Div., Rept. SID-62-993-VOL-5-APP-B, Downey, CA, 1962.
[55] Wool, M. R., "Passive Nosetip Technology (PANT) Program, Volume 10: Summary of Experimental and Analytical Results," Space and Missile Systems Organization TR-74-86-Vol-X, Los Angeles AFB, CA, Jan. 1975.
[56] Abbett, M. J., Anderson, A. D., Cooper, L., Dahm, T. J., Kelly, J., Overly, P., and Sandhu, S., "Passive Nosetip Technology (PANT) Program, Volume 20: Investigation of Flow Phenomena over Reentry Vehicle Nosetips," Space and Missile Systems Organization, TR-74-86-Vol-XX, Los Angeles AFB, CA, Aug. 1975.
[57] Jackson, M. D., "Passive Nosetip Technology (PANT) Program, Volume 15: Roughness Induced Transition on Blunt Axisymmetric Bodies," Space and Missile Systems Organization TR-74-86-Vol-XV, Los Angeles AFB, CA, Apr. 1974.
[58] Grabow, R. M., and White, C. O., "Surface Roughness Effects on Nosetip Ablation Characteristics," AIAA Paper 74-513, June 1974.
[59] Eitman, D. A., and DeMichaels, J. E., "Performance Technology Program (PTP-S II)," Vol. 10, U.S. Air Force Ballistic Missile Office, TR 80-40 BMO, Norton AFB, CA, Jan. 1980.
[60] Morkovin, M. V., "Bypass Transition to Turbulence and Research Desiderata," *Transition in Turbines*, NASA CP-2386, May 1984, pp. 161–199.
[61] Morkovin, M. V., "Critical Evaluation of Transition from Laminar to Turbulent Shear Layers with Emphasis on Hypersonically Traveling

Bodies," U.S. Air Force Flight Dynamics Lab., TR 68-149, Wright–Patterson AFB, OH, Mar. 1969.
[62] Stetson, K. F., "Boundary-Layer Transition on Blunt Configurations," NASA Johnson Space Center, Rept. JSC-26528, Houston, TX, Feb. 1994.
[63] Murphy, J. D., and Rubesin, M. W., "Re-Evaluation of Heat-Transfer Data Obtained in Flight Tests of Heat-Sink Shielded Re-Entry Vehicles," *Journal of Spacecraft and Rockets*, Vol. 3, No. 1, Jan. 1966, pp. 53–60. doi:10.2514/3.28385
[64] Murphy, J. D., and Rubesin, M. W., "An Evaluation of Free-Flight Test Data for Aerodynamic Heating from Laminar, Turbulent, and Transitional Boundary Layers Part 2: The X-17 Re-Entry Body," NASA, CR-70931, Apr. 1965.
[65] Balgeman, E. J., Cassell, G., Dension, M. R., and Tellep, D. M., "X-17 Re-Entry Test Vehicle: R-2 Final Flight Report," Missile Systems Div., Lockheed Aircraft Corp., Rept. MSD-3003, Sunnyvale, CA, Apr. 1957.
[66] Wisniewski, R. J., "Correlation of Boundary-Layer Transition Results on Highly Cooled Blunt Bodies," NASA, TM-X-412, Oct. 1960.
[67] Potter, L. J., and Whitfield, J. D., "The Relation Between Wall Temperature and the Effect of Roughness on Boundary-Layer Transition," *Journal of the Aerospace Sciences*, Vol. 28, No. 8, Aug. 1961, pp. 663–664.
[68] Finson, M. L., "An Analysis of Nosetip Boundary Layer Transition Data," Physical Sciences, Inc., Rept. PSI-TR-52, Woburn, MA, Aug. 1976; also U.S. Air Force Office of Scientific Research, Rept. AFOSR-TR-76-1106, Wright–Patterson AFB, OH, 1976.
[69] Finson, M. L., Pirri, A. N., Nebolsine, P. E., Simons, G. A., and Wu, P. K. S., "Advanced Reentry Aeromechanics," Physical Sciences, Inc., Rept. PSI-TR-115, Woburn, MA, Jan. 1978; also U.S. Air Force Office of Scientific Research, Rept. AFOSR-TR-78-0607TR, Wright–Patterson AFB, OH, 1978.
[70] Seiff, A., Sommer, S., and Canning, T., "Some Experiments at High Supersonic Speeds on the Aerodynamic and Boundary-Layer Transition Characteristics of High-Drag Bodies of Revolution," NACA RM-A56I05, Jan. 1957.
[71] Cooper, M., and Mayo, E., "Measurements of Local Heat Transfer and Pressure on Six 2-Inch-Diameter Blunt Bodies at a Mach Number of 4.95 and at Reynolds Numbers per Foot Up to $81 \times 10(\exp 6)$," NASA TM-1-3-59L, Mar. 1959.
[72] Stetson, K. F., "Nosetip Bluntness Effects on Cone Frustum Boundary Layer Transition in Hypersonic Flow," AIAA Paper 83-1763, July 1983.
[73] Bandettini, A., and Isler, W. E., "Boundary-Layer Transition Measurements on Hemispheres of Various Surface Roughnesses in a Wind Tunnel at Mach Numbers from 2.48 to 3.55," NASA TM-12-25-58A, Mar. 1959.
[74] Cooper, M., Mayo, E., and Julius, J., "The Influence of Low Wall Temperature on Boundary-Layer Transition and Local Heat Transfer on 2-Inch-Diameter Hemispheres at a Mach Number of 4.95 and at a Reynolds Numbers per Foot of 73.2×10^6," NASA TN-D-391, July 1960.
[75] Deveikis, W. D., and Walker, R. W., "Local Aerodynamic Heat Transfer and Boundary-Layer Transition on Roughened Sphere-Ellipsoid Bodies at Mach Number 3.0," NASA, TN-D-907, Aug. 1961.
[76] Jackson, M. W., and Czarnecki, K. R., "Boundary-Layer Transition on a Group of Blunt Nose Shapes at a Mach Number of 2.20," NASA, TN-D-932, July 1961.
[77] Boudreau, A. H., "Correlation of Artificially Induced Boundary-Layer Transition Data at Hypersonic Speeds," *Journal of Spacecraft and Rockets*, Vol. 18, No. 2, Mar.–Apr. 1981, pp. 152–156. doi:10.2514/3.28053
[78] Dunavant, J. C., and Stone, H. W., "Effect of Roughness on Heat Transfer to Hemisphere Cylinders at Mach Numbers 10.4 and 11.4," NASA, TN-D-3871, Mar. 1967.
[79] Van Driest, E. R., Blumer, C. B., and Wells, C. S., Jr., "Boundary Layer Transition on Blunt Bodies—Effects of Roughness," *AIAA Journal*, Vol. 5, Oct. 1967, pp. 1913–1915. doi:10.2514/3.4337
[80] Van Driest, E. R., and Blumer, C. B., "Boundary Layer Transition on Cones and Spheres at Supersonic Speeds–Effects of Roughness and Cooling," U.S. Air Force Office of Scientific Research, Rept. 67-2048, Wright–Patterson AFB, OH, July 1967.
[81] Varwig, R. L., "Effect of Roughness on Heating at the Forward Surface of a Sphere at Mach 5," Space and Missile Systems Organization, Rept. TR-70-229, Los Angeles AFB, CA, Apr. 1970.
[82] Ross, D. H., Ellinwood, J. W., and Varwig, R. L., "Hypersonic Shock Tunnel Transition Studies," Boundary Layer Transition Workshop, Aerospace Corp. Paper 8, Dec. 1971; also Aerospace Corp., Rept. TOR-0172(S2816-16)-5, San Bernardino, CA, Dec. 1971.
[83] Coats, J. D., "Investigation of the Effects of Nose Bluntness on Natural and Induced Boundary-Layer Transition on Axisymmetric Bodies in Supersonic Flow," Arnold Engineering Development Center, AEDC-TR-73-36, Tullahoma, TN, Feb. 1973.
[84] Creel, T. R., Jr., "Experimental Investigation at Mach 8 of the Effects of Projections and Cavities on Heat Transfer to a Model of the Viking Aeroshell," NASA TM-X-2941, Apr. 1974.
[85] Laderman, A. J., "Effect of Surface Roughness on Blunt Body Boundary-Layer Transition," *Journal of Spacecraft and Rockets*, Vol. 14, No. 4, Apr. 1977, pp. 253–255. doi:10.2514/3.27968
[86] Demetriades, A., Laderman, A. J., Von Seggern, L., Hopkins, A. T., and Donaldson, J. C., "Effect of Mass Addition on the Boundary Layer of a Hemisphere at Mach 6," *Journal of Spacecraft and Rockets*, Vol. 13, No. 8, Aug. 1976, pp. 508–509. doi:10.2514/3.27924
[87] Richards, B. E., and DiCristina, V., "Heat Transfer Studies on Ablation Protected Nosetips at Reentry Simulated Conditions," AIAA Paper 77-781, June 1977.
[88] Reda, D. C., "Boundary-Layer Transition Experiments on Sharp, Slender Cones in Supersonic Free Flight," *AIAA Journal*, Vol. 17, No. 8, Aug. 1979, pp. 803–810. doi:10.2514/3.61231
[89] Reda, D. C., "Comparative Transition Performance of Several Nosetip Materials at Defined by Ballistics-Range Testing," *ISA Transactions*, Vol. 19, No. 1, Jan. 1980, pp. 83–98; also *Proceedings of the 25th International Instrumentation Symposium*, Instrument Society of America, Pittsburgh, PA, May 1979, pp. 89–104.
[90] Todisco, A., Reeves, B., Siegelman, D., and Mascola, R., "Boundary Layer Transition on Blunt Axisymmetric Nosetips Induced by Single and Multiple Craters," AIAA Paper 81-1087, June 1981.
[91] Wassel, A. T., Shih, W. C. L., and Courtney, J. F., "Roughness Induced Transition and Heat Transfer Augmentation in Hypersonic Environments," AIAA Paper 84-0631, Mar. 1984.
[92] Schöler, H., "Thermal Imaging on Missiles in Hypersonic Flow," *Missile Aerodynamics*, AGARD CP-493, Neuilly-sur-Seine, France, Apr. 1990, p. 29.
[93] Holden, M. S., "Studies of Potential Fluid-Mechanical Mechanisms for Enhanced Stagnation-Point Heating," *Thermophysical Aspects of Reentry Flows*, edited by J. N. Moss and C. D. Scott, Vol. 103, Progress in Astronautics and Aeronautics, AIAA, New York, 1986, pp. 281–309.
[94] Holden, M. S., and Rodriguez, K. M., "Studies of Shock/Shock Interaction on Smooth and Transpiration-Cooled Hemispherical Nosetips In Hypersonic Flows," NASA, CR-189585, Apr. 1992; also Calspan Advanced Technology Center, TR 7931, Buffalo, NY, Apr. 1992.
[95] Zanchetta, M. A., and Hillier, R., "Laminar Turbulent Transition at Hypersonic Speeds: The Effects of Nose Blunting," *2nd European Symposium on Aerothermodynamics for Space Vehicles*, ESA, Paris, Feb. 1995, pp. 207–212.
[96] Zanchetta, M., "Kinetic heating and transition studies at hypersonic speeds," Ph.D. Thesis, Dept. of Aeronautics, Imperial College of Science, Technology, and Medicine, London, Apr. 1996.
[97] Carbonaro, M., Charbonnier, J.-M., and Deconinck, H., "Hypersonic Aerothermodynamics at VKI," *Aerothermodynamics and Propulsion Integration for Hypersonic Vehicles*, AGARD, R-813, Neuilly-sur-Seine, France, Oct. 1996.
[98] Charbonnier, J.-M., and Boerrigter, H., "Roughness-Induced Transition in Hypersonic Flow," *Space Scientific Research in Belgium*," Vol. 4, Mar. 1996, pp. 43–44.
[99] Boerrigter, H., and Charbonnier, J.-M., "Roughness-Induced Transition in Hypersonic Flow," *Space Scientific Research in Belgium*," Vol. 4, Mar. 1996, pp. 51–52.
[100] Bertin, J. J., Stetson, K. F., Bouslog, S. A., and Caram, J. M., "Effects of Isolated Roughness Elements on Boundary-Layer Transition for Shuttle Orbiter," *Journal of Spacecraft and Rockets*, Vol. 34, No. 4, July–Aug. 1997, pp. 426–436. doi:10.2514/2.3254
[101] Charbonnier, J.-M., Dieudonne, W., and Boerrigter, H., "Simulation of Transitional and Turbulent Boundary Layer Flow on Blunted Geometry in Hypersonic Flow," *3rd European Symposium on Aerothermodynamics for Space Vehicles*, ESA, Paris, Nov. 1998, pp. 291–297.
[102] Paris, S., Fletcher, D., Cerignat, L., and Garzon, A., "Roughness-

Induced Transition for Flight Experiments," *Fourth International Symposium on Atmospheric Reentry Vehicles and Systems* [CD-ROM], Association Aéronautique et Astronautique de France, Paris, Mar. 2005.

[103] Horvath, T. J., McGinley, C. B., and Hannemann, K., "Blunt Body Near-Wake Flow Field at Mach 6, AIAA Paper 96-1935, June 1996.

[104] Cheatwood, F. M., Merski, N. R., Riley, C. J., and Mitcheltree, R. A., "Aerothermodynamic Environment Definition for the Genesis Sample Return Capsule," AIAA Paper 2001-2889, June 2001.

[105] Tang, Chun Y., and Wright, M. J., "Analysis of the Forebody Aeroheating Environment During Genesis Sample Return Capsule Reentry," AIAA Paper 2007-1207, Jan. 2007.

[106] Hollis, B. R., and Liechty, D. S., "Boundary-Layer Transition Correlations and Aeroheating Predictions for Mars Smart Lander," AIAA, Paper 2002-2745, June 2002.

[107] Edquist, Karl T., Liechty, Derek S., Hollis, B. R., Alter, S. J., and Loomis, M. P., "Aeroheating Environments for a Mars Smart Lander," *Journal of Spacecraft and Rockets*, Vol. 43, No. 2, Mar.–Apr. 2006, pp. 330–339. doi:10.2514/1.19431

[108] Edquist, K. T., Dyakonov, A. A., Wright, M. J., and Tang, C. Y., "Aerothermodynamic Environments Definition for the Mars Science Laboratory Entry Capsule," AIAA, Paper 2007-1206, Jan. 2007.

[109] Hollis, B. R., and Collier, A. S., "Turbulent Aeroheating Testing of Mars Science Laboratory Entry Vehicle in Perfect-Gas Nitrogen," AIAA, Paper 2007-1208, Jan. 2007.

[110] Lafferty, J. F., and Norris, J. D., "Measurements of Fluctuating Pitot Pressure, 'Tunnel Noise' in the AEDC Hypervelocity Wind Tunnel No. 9," AIAA Paper 2007-1678, Feb. 2007.

[111] Schrijer, F. F. J., Scarano, F., Van Oudheusden, B. W., and Bannink, W. J., "Experiments on Hypersonic Roughness Induced Transition by Means of Infrared Thermography," *5th European Symposium on Aerothermodynamics for Space Vehicles*, ESA, Paris, Nov. 2004, pp. 255–260.

[112] Reda, D. C., Wilder, M. C., Bogdanoff, D. W., and Olejniczak, J., "Aerothermodynamic Testing of Ablative Reentry Vehicle Nosetip Materials in Hypersonic Ballistic-Range Environments," AIAA, Paper 2004-6829, Nov. 2004.

[113] Reda, D. C., Wilder, M. C., Bogdanoff, D. W., and Prabhu, D., "Transition Experiments on Blunt Bodies with Distributed Roughness in Hypersonic Free Flight," AIAA Paper 2007-0306, Jan. 2007.

[114] Murphy, K. J., Borg, S. E., Watkins, A. N., Cole, D. R., and Schwartz, R. J., "Testing of the Crew Exploration Vehicle in NASA Langley's Unitary Plan Wind Tunnel," AIAA Paper 2007-1005, Jan. 2007.

[115] Braslow, A. L., Hicks, R. M., and Harris, R. V., Jr., "Use of Grit-Type Boundary-Layer Transition Trips on Wind-Tunnel Models," NASA TN-D-3579, Sept. 1966.

[116] Ross, J. C., "Aerodynamic Testing in Support of Orion Spacecraft Development," AIAA Paper 2007-1004, Jan. 2007.

[117] Sommer, S. C., Short, B. J., and Compton, D. L., "Free-Flight Measurements of Static and Dynamic Stability of Models of the Project Mercury Re-Entry Capsule at Mach Numbers 3 and 9.5," NASA TM-X-373, Aug. 1960.

R. Kimmel
Associate Editor